Chemical Geology 662 (2024) 122218

Contents lists available at ScienceDirect

Chemical Geology

journal homepage: www.elsevier.com/locate/chemgeo

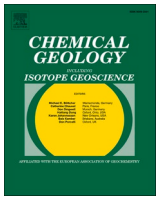

Why are oceanic arc basalts Ca-rich and Ni-poor? Insights from olivine-hosted melt inclusions from Kibblewhite Volcano in the Kermadec arc

Yasuhiro Hirai [a,b,c,*], Yoshihiko Tamura [b], Takeshi Hanyu [b], Qing Chang [b], Christian Timm [d], Kaj Hoernle [d,e]

[a] Division of Natural System, Kanazawa University, 920-1192, Ishikawa, Japan
[b] Research Institute for Marine Geodynamics, Japan Agency for Marine-Earth Science and Technology (JAMSTEC), 237-0061, Kanagawa, Japan
[c] Yoshida Junior High School, 369-1503 Saitama, Japan
[d] Research Institute for the Igneous and Hydrothermal System of the Ocean Floor, GEOMAR Helmholtz Centre for Ocean Research, 2418 Kiel, Germany
[e] Institute of Geosciences, Kiel University, 24118 Kiel, Germany

ARTICLE INFO

Editor: Claudia Romano

Keywords:
Petrology
Kermadec arc
Melt inclusion
Primary melt
Arc ankaramite
Melt-mantle interaction

ABSTRACT

Ankaramites, which are clinopyroxene-rich basalts with primitive whole-rock compositions (Mg# >65), are common in oceanic arcs and are characterized by high whole-rock CaO/Al_2O_3 (>1.0) ratios and olivine crystals with anomalously low nickel contents (<0.2 wt% NiO). These geochemical characteristics cannot be explained by the melting of ordinary mantle peridotite. However, their origin is critical for understanding the formation of primary magmas in oceanic arcs. Here, we investigated olivine-hosted melt inclusions (MIs) from ankaramites and magnesian andesites of the Kibblewhite Volcano in the Kermadec arc. The MIs from the ankaramites have similar major and trace element characteristics to the host rocks, indicating that the ankaramites did not result from an accumulation of mafic minerals but rather represent the primary magma in the Kibblewhite Volcano. The MIs from the magnesian andesites were hosted in forsteritic olivine xenocrysts with a wide range of NiO contents ($Fo_{90–92}$; 0.13–0.39 wt% NiO) and have similar major element compositions to the ankaramites but exhibit a wide range of CaO/Al_2O_3 (0.85–1.54). The trace element characteristics of the MIs from the magnesian andesites do not match those of the host rocks, indicating that they are not primary melts of the magnesian andesites but primitive basaltic melts generated before the magnesian andesites formed.

Interestingly, the CaO/Al_2O_3 ratio of MIs from the magnesian andesites was negatively correlated with the NiO content of their host olivines. This correlation suggests that the composition of the primary basaltic magmas of the Kibblewhite Volcano changed continuously from peridotite-derived to ankaramitic. This correlation could not be explained by grain-scale process, crustal anatexis, or contribution of slab-derived carbonate-rich fluids. Instead, we propose that this correlation can be explained by the interaction of the ascending primary basaltic melts with the lithospheric mantle. During melt-mantle interaction, the assimilation of clinopyroxene and fractionation of olivine and orthopyroxene caused the CaO/Al_2O_3 ratio to increase in the melt and the Ni content to decrease. Furthermore, because the magnesian andesites have low CaO/Al_2O_3 ratios and could be derived from a clinopyroxene-poor mantle lithology, the interaction between the melt and mantle may also be closely related to the origin of the magnesian andesites at Kibblewhite Volcano. This interpretation provides a new perspective on the origin of the oceanic arc ankaramites and why primary andesitic and basaltic magmas coexist in the Kibblewhite Volcano.

* Corresponding author at: Division of Natural System, Kanazawa University, 920-1192, Ishikawa, Japan.
E-mail address: deep.forest.alliance@gmail.com (Y. Hirai).

https://doi.org/10.1016/j.chemgeo.2024.122218
Received 23 February 2024; Received in revised form 30 May 2024; Accepted 9 June 2024
Available online 11 June 2024

1. Introduction

Understanding the formation of primary melts is key to elucidating magmatic processes in subduction zones. Primary melts in oceanic arcs have attracted the attention of scientists because the effects of crystal fractionation and crustal contamination are typically smaller in such magmas due to the thinner crust in these areas. In the last decade, we have reported primitive basalts, which have high whole-rock Mg-numbers (Mg#, 100 Mg/[Mg + Fe] >65) and contain olivines with high forsterite contents (Fo, 100 Mg/[Mg + Fe] >90), from several oceanic arc volcanoes such as the Pagan Volcano in the Mariana arc (Tamura et al., 2014), the Nishinoshima Volcano in the Ogasawara arc (Tamura et al., 2019a) and the Kibblewhite Volcano in the Kermadec arc (Hirai et al., 2023). These primitive basalts contained abundant olivine and clinopyroxene crystals, with clinopyroxene dominating the phenocrysts. Such clinopyroxene-rich basalts were also sampled from the Doyo Seamount near the Nishinoshima Volcano in the Ogasawara arc by SHINKAI 6500 (Tamura et al., 2019b) and from the unnamed seamount (DR129) in the Kermadec arc by dredge sampling of the R/V SONNE during the SO-255 expedition (Hoernle et al., 2017). Thus, clinopyroxene-rich basalts could be representative rocks/volcanics in oceanic arcs. Hereafter, we refer to these primitive basalts as "oceanic arc ankaramites," in accordance with the naming of clinopyroxene-rich basalts observed in island-arc settings as "arc ankaramites." (Barsdell and Berry, 1990).

However, some debate exists on whether oceanic ankaramites can truly represent mantle-derived primary magmas in oceanic arcs because they have two geochemical characteristics that cannot be in equilibrium with mantle peridotite. First, they are too Ca-rich to be generated by the melting of mantle peridotite. Experimental lherzolite melts generally have $CaO/Al_2O_3 < 1.0$; however, oceanic arc ankaramites show $CaO/Al_2O_3 > 1.0$, even with similar Mg# (Fig. 1a). The second reason is the anomalously low NiO content of their olivines. Olivines in mantle peridotites generally have 0.4 ± 0.1 wt% NiO at high forsterite content ($Fo_{90–93}$), but oceanic arc ankaramites contain olivines with <0.25 wt% NiO, even with similar forsterite contents (Fig. 1b). Even compared with the olivine phenocrysts of mid-ocean ridge basalts (MORB; Sobolev et al., 2007), which are thought to be derived from the melting of ordinary mantle peridotites, olivine in oceanic arc ankaramites is clearly poor in Ni (Fig. 1b). This indicates that the primary melts that form oceanic ankaramites already have low Ni contents. High CaO/Al_2O_3 and low Ni contents are the basic properties of island-arc primitive basalts (Green and Falloon, 1998), but how these geochemical characteristics are produced remains poorly understood.

Melt inclusions (MIs) are a powerful tool for directly determining primary melt composition. The purpose of this study was to reveal the primary melt compositions of Kibblewhite Volcano using olivine-hosted MIs. Around this volcano, we sampled ankaramites and magnesian andesites produced by the hydrous melting of mantle peridotite at low pressure (Hirai et al., 2023). We analyzed the MIs hosted in olivine phenocrysts from the ankaramites and those hosted in olivine xenocrysts from the magnesian andesites. Based on the results, this study addressed the following questions. (1) Are these MIs primary melts from the Kibblewhite Volcano? (2) What is the origin of the high CaO/Al_2O_3 ratio and low Ni content in the ankaramites? (3) Why do ankaramites and magnesian andesites coexist?

2. Samples

2.1. Geological background

The Kermadec arc is produced by the subduction of the Pacific Plate beneath the Australian Plate and is one of the most hydrothermally and volcanically active oceanic arcs on Earth (de Ronde et al., 2007), extending from the north of New Zealand towards Tonga. The volcanic front of the Kermadec arc is built on a ~ 12 km thick crust (Bassett et al., 2016), which is one of the thinnest oceanic crusts underlying volcanic arcs. Kibblewhite Volcano is a submarine volcano located approximately 500 km northeast of Auckland, North Island, New Zealand. Kibblewhite Volcano consists of andesite, dacites, and rhyolite and is surrounded by several neighboring cones consisting of basalts (Hirai et al., 2023; Wright et al., 2006). Host rocks of the MIs studied here were collected from the Kibblewhite Volcano and a neighboring cone by dredge sampling conducted by the R/V SONNE SO-255 expedition in 2017 (Hirai et al., 2023; Hoernle et al., 2017). A bathymetric map of the Kibblewhite Volcano and the sampling locations of the host rocks are shown in Fig. S1.

MIs were obtained from two types of host rock: ankaramites and magnesian andesites. The ankaramites were collected from the cinder cone named 'KI4,' neighboring at ~10 km southeastern of the Kibblewhite Volcano, whereas the magnesian andesites were collected from the northeastern flank of the Kibblewhite Volcano. Hirai et al. (2023) reported detailed petrology of the host rocks. The petrography and geochemistry of the host rocks are described briefly in Section 2.2 and Section 2.3.

2.2. Ankaramites

Ankaramites from the Kibblewhite Volcano contain a large proportion of olivine (9–17 vol%) and clinopyroxene (21–32 vol%) crystals that show a wide range of compositions ($Fo_{80–92}$ for olivine and Mg# = 79–94 for clinopyroxene). Partially crystallized MIs were identified by thin-section observations, especially in large olivine crystals. In this study, the olivines containing MIs were extracted from two ankaramite samples, DR28–10 and DR28–25, which had whole-rock compositions of primitive basalts (50.4–50.6 wt% SiO_2; 13.1–13.5 wt% MgO; Mg# = 71.8–72.2). Based on Mg#, the ankaramites appear to be in equilibrium with mantle peridotite, but they show $CaO/Al_2O_3 > 1.0$ (Fig. 1a); thus, they cannot have been produced by ordinary mantle melting.

2.3. Magnesian andesites

The magnesian andesites have an aphyric texture and are composed of olivine and clinopyroxene microphenocrysts (0.2–0.4 mm) that appear to be in equilibrium with the whole-rock compositions ($Fo_{84–86}$ for olivine and Mg# = 82–87 for clinopyroxene), although they also contain 1–2 vol% of large olivine crystals (>0.5 mm) (Fig. S2a). Hirai et al. (2023) interpreted these large olivines as xenocrysts, as they have forsteritic cores ($Fo_{90–93}$) that cannot be in equilibrium with magnesian andesites and are surrounded by thin rims with compositions similar to those of the microphenocrysts in the magnesian andesites ($Fo_{84–86}$). These petrographic features indicate that the large olivines crystallized from another primitive magma and were then incorporated into the magnesian andesites as xenocrysts. We used DIPRA software to analyze the diffusion process of olivine crystals (Girona and Costa, 2013) and estimated their residence time in the melt as between 5 and 40 d (15 d on average; $n = 14$) (Fig. S2b).

Through thin-section observation, we identified partially crystallized MIs composed of glass and clinopyroxene in some olivine xenocrysts (Fig. S2a). These host olivine xenocrysts were selectively extracted and analyzed according to the analytical procedures described in Section 3.

3. Methods

3.1. Analytical procedures

Fist-sized rock samples were disintegrated using SELFRAG® high-voltage pulse power fragmentation at the Japan Agency for Marine-Earth Science and Technology (JAMSTEC). We handpicked olivine crystals containing MIs under a binocular stereomicroscope. Olivines from the magnesian andesites were sieved to extract those xenocrysts with a size of >0.5 mm. All the inclusions selected here were partially

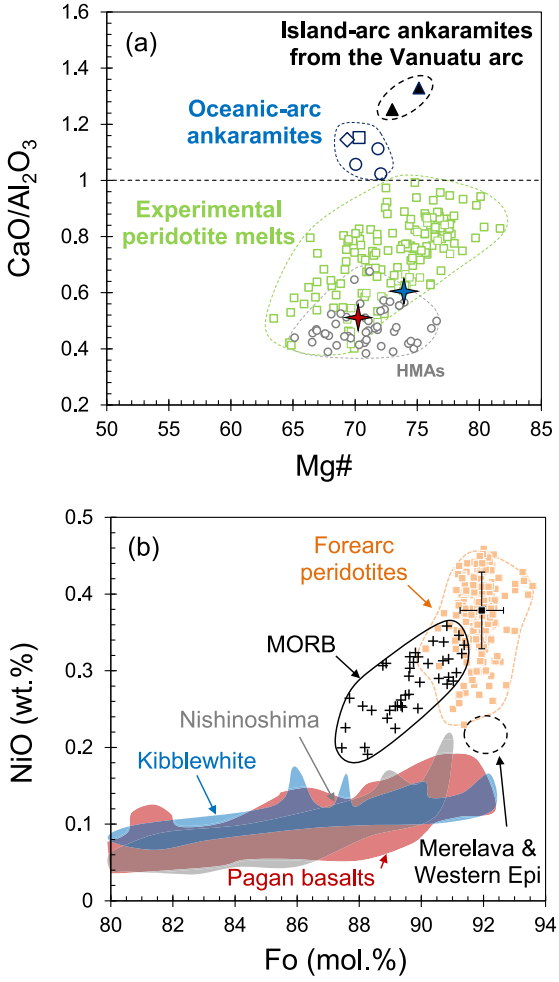

(caption on next column)

Fig. 1. Geochemical features of the oceanic arc ankaramites that cannot be explained by melting of mantle peridotite. (a) Variation of CaO/Al_2O_3 versus Mg#. Open green squares are experimental partial melts of various lherzolites at 0.5–2.0 GPa in dry and wet conditions (Baker and Stolper, 1994; Falloon and Green, 1988, Falloon and Green, 1987; Grove et al., 2003; Hirose, 1997; Hirose and Kawamoto, 1995; Hirose and Kushiro, 1993; Kushiro, 1996; Laporte et al., 2004; Villiger et al., 2004; Wasylenki et al., 2003). Filled triangles are the arc ankaramites from the Vanuatu arc (Merelava and Western Epi Volcanoes in the Vanuatu arc; Barsdell, 1988; Barsdell and Berry, 1990). Blue symbols are the oceanic arc ankaramites from oceanic arcs (diamond: COB1-type basalt of the Pagan Volcano in the Mariana arc; Tamura et al., 2014; square: Nishinoshima Volcano in the Ogasawara arc; Tamura et al., 2019a; circle: Kibblewhite Volcano in the Kermadec arc; Hirai et al., 2023). Open gray circles are high-Mg# andesites from subduction zones (HMAs: Kamchatka; Bryant et al., 2011; Nishizawa et al., 2017; SW Japan: Tatsumi and Ishizaka, 1982; Taupo Volcanic Zone: Heyworth et al., 2007; Cascade: Baker et al., 1994; Grove et al., 2002; Ruscitto et al., 2011; Central Mexican volcanic belt: Blatter and Carmichael, 1998; Straub et al., 2014; Western Aleutian: Yogodzinski et al., 1994). Red and blue crosses show the Kibblewhite HMAs that are estimated primary melt compositions for the magnesian andesites from the olivine addition and olivine + clinopyroxene addition models (Hirai et al., 2023). (b) Variations in NiO versus forsterite content (Fo: =100 Mg/[Mg + Fe]) of olivines in the oceanic arc ankaramites. Olivines in the oceanic arc ankaramites show lower NiO contents (<0.23 wt%) than those of the forearc peridotites (Ishii et al., 1992), even at high Fo content ($Fo_{90–92}$). Crosses are the olivines obtained from mid-ocean ridge basalts (MORB) by Sobolev et al. (2007). Data sources for the oceanic arc ankaramites are the same as for Fig. 1a. (For interpretation of the references to colour in this figure legend, the reader is referred to the web version of this article.)

crystallized (Fig. S3a); thus, a re-homogenization experiment was necessary to analyze these MIs. For the analyses, the MIs were homogenized using a heating stage (Linkam TS1500). Double-polished olivine grains were heated in an Ar atmosphere and monitored under a microscope until the inclusions were completely molten. After maintaining homogenization temperatures (1180–1240 °C in the measurement period) for 5 min, the samples were rapidly quenched by extracting them from the heating furnace. After the heating experiments, complete homogenization of each melt inclusion was confirmed under a microscope (Fig. S3b). MIs that burst or were crosscut by cracks during heating were discarded.

Major element compositions of the host olivines were determined using an electron microprobe analyzer (EPMA; JEOL JXA-8500F Superprobe) equipped with five wavelength-dispersive spectrometers at JAMSTEC. Host olivines were analyzed using a 20 kV accelerating voltage, 25 nA beam current, and 5 μm beam spot size. The counting times were 20 s at the peak, 10 s in the background for Si, Ti, Al, Fe, and Mg, 100 s at the peak, and 50 s in the background for Mn, Ca, and Ni. Two standard deviations for MnO, CaO, and NiO in analyzing in-house olivine standards were ± 0.006, ±0.011, and ± 0.010 wt% (n = 9), respectively, during the measurement period. The measured chemical compositions of the host olivines are presented in Table S1.

H_2O contents of the homogenized and unexposed MIs were determined using micro-Fourier Transform Infra-Red (FTIR) spectroscopy based on the method of Nichols and Wysoczanski (2007). Micro-FTIR spectroscopy was performed using a Varian FTS Stingray 7000 Micro Image Analyzer spectrometer at JAMSTEC. Total H_2O concentration was calculated using the vibration band at approximately 3500 cm^{-1}. The thicknesses of the unexposed MIs in the olivine were obtained from FTIR spectra (Nichols and Wysoczanski, 2007). Molar absorptivity coefficients of 63 ± 5 l/mol·cm (Dixon et al., 1988) were used to calculate concentrations from the height of the peaks above a linear baseline. Glass densities were calculated from the oxide compositions and subsequently measured by EPMA using the model of Lange and Carmichael (1987). No peaks were observed at approximately 1435 cm^{-1} and 1515 cm^{-1} in any of the spectra of the samples studied here, indicating the absence of CO_2 in the glasses of homogenized MIs. After the micro-FTIR

analyses, the olivine grains were mounted on acrylic resin and polished to expose the homogenized glassy MIs on the surface for microprobe and laser ablation analyses.

Major element compositions and S and Cl contents of the homogenized MIs were analyzed with a 15 kV accelerating voltage, 10 nA beam current, and 10 μm beam spot size. Counting times were 10 s at the peak and 5 s in the background for Na and K, 20 s at the peak and 10 s in the background for Si, Ti, Al, Fe, Mg, Ca, and P, and 100 s at the peak and 50 s in the background for Cl and S. Na and K were measured first to avoid 'Na-loss' during measurement (Morgan and London, 1996).

Trace element compositions of MIs were determined using laser-ablation ICP-MS. A 200 nm femtosecond laser (OK Laboratory; OK-Fs2000K) coupled with a sector-field ICP-MS (Thermo Fisher Scientific; Element XR) at JAMSTEC was used for the measurements. The ablation pit was set to a diameter of 20–30 μm and a depth of 20 μm. For normalization, a GSD-1G basalt standard glass from the United States Geological Survey (USGS) was measured after every five unknown samples. For quality control, a BHVO-2G international glass standard from the USGS was measured repeatedly. The major, volatile (S, Cl), and trace element compositions of the olivine-hosted MIs are shown in Table S2.

3.2. Correction for post-entrapment crystallization

The MIs analyzed here were compositionally modified by a post-entrapment crystallization (Kent, 2008) and "Fe-loss" process (Danyushevsky et al., 2000). Most of the homogenized MIs from the Kibblewhite Volcano showed a low Mg# (=100 × Mg/[Mg + Fe]), which would not be in equilibrium with the host olivines (Fig. S4a). The low Mg# of the MIs could have been caused by the post-entrapment crystallization of olivine on the walls of the inclusions during pre-eruptive cooling (Kent, 2008). FeO contents in MIs are also variable during pre-eruptive cooling, caused by re-equilibration of the MIs with the host olivines, referred to as "Fe-loss" (Danyushevsky et al., 2000). The initial FeO contents of the MIs were estimated from the Fo-FeO diagram (Fig. S4b). The effect of Fe-loss was the smallest in the sample with the lowest Fo content, as the extent of the compositional change caused by Fe-loss depends on the temperature interval between trapping and natural quenching (Danyushevsky et al., 2000). MIs hosted in the lowest-Fo olivines of the ankaramites (Fo_{83}) and magnesian andesites (Fo_{86}) were approximately 9 wt% FeO, consistent with the highest FeO contents of the MIs in the high-Fo olivines (Fig. S4b). This indicates that the MIs initially contained ~9 wt% FeO because the FeO contents in primitive basaltic melts are not significantly changed by olivine (+ clinopyroxene) crystallization. Therefore, the initial FeO content of the Mis was assumed to be 9 wt%.

We corrected for the effect of post-entrapment crystallization and Fe-loss in the MIs using the "Petrolog" software version 3.1.1.3 (Danyushevsky and Plechov, 2011). This software can restore the primary melt composition by iteratively adding equilibrium olivine with correction for the effect of Fe-loss by assuming the initial FeO content. Consequently, 0–21% olivine was added to the homogenized MIs for correction. Trace element compositions were corrected using olivine-melt partition coefficients ($D_{element}$) estimated from the MgO content of the MIs. Applied values for Sc and Cr ($D_{Sc} = 0.15$ and $D_{Cr} = 1.0$) were estimated using the model of Bédard (2005). Applied values for Ni ($D_{Ni} = 12$) were estimated using the model of Hart and Davis (1978). D values for Ba, Th, Nb, and rare earth elements (REEs) were assumed to be zero because these elements have sufficiently low D values (<0.1; Bédard, 2005). After correction for post-entrapment crystallization and "Fe-loss," melt inclusion compositions are shown in Table S3. The corrected compositions are used in Section 4.

4. Results

4.1. Host olivine chemistry

Fig. 2 shows the variation in NiO and CaO versus the Fo content and Mg# of the host olivines obtained from the ankaramites and magnesian andesites. Host olivines from the ankaramites show high Fo contents ($Fo_{90–92}$), except for one grain (Fo_{83}), with uniformly low NiO contents (<0.2 wt% NiO). The CaO contents of the host olivines are similar to those of olivines from peridotite-derived melt (Gavrilenko et al., 2016). These chemical characteristics of the host olivines are consistent with thin-section analyses of olivines in ankaramites (Hirai et al., 2023). Host olivines from the magnesian andesites showed high Fo contents ($Fo_{90–92}$), except for one grain (Fo_{86}). The host olivines were characterized by variable NiO contents at a given Fo content (0.12–0.39 wt% NiO at $Fo_{90–92}$), which is consistent with the thin section analysis of olivine xenocrysts in magnesian andesites (Hirai et al., 2023). The CaO contents of the host olivines were also consistent with those of the olivine xenocrysts in the thin sections. These compositional similarities

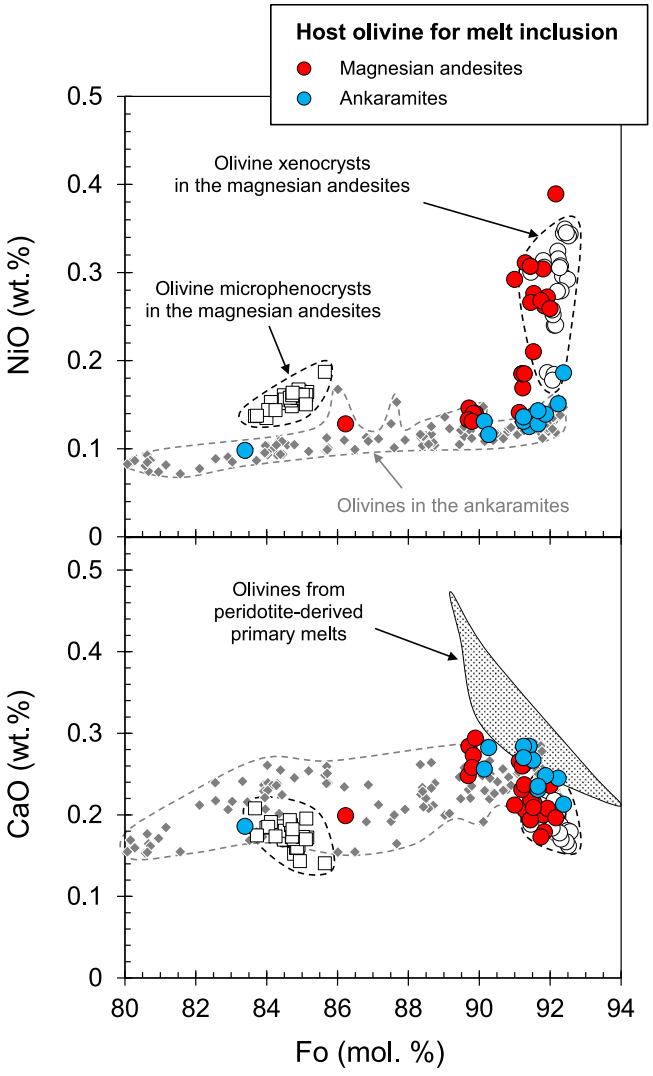

Fig. 2. Variations of NiO and CaO with forsterite contents of host olivines. Open circles and squares represent olivine xenocrysts and olivine microphenocrysts in the magnesian andesites (Hirai et al., 2023). Gray diamonds show olivines in ankaramites from the neighboring cone KI4, the Kibblewhite Volcano (Hirai et al., 2023). The shaded area represents the CaO contents of olivines from peridotite-derived primary melts in dry conditions (Gavrilenko et al., 2016).

indicate that the host olivines of the MIs analyzed here are xenocrysts incorporated into the magnesian andesites prior to their eruption.

4.2. Melt inclusion chemistry

4.2.1. Major elements

After correcting for post-entrapment crystallization, the compositions of MIs from the ankaramites and magnesian andesites ranged from basalt to basaltic andesite (50–53 wt% SiO_2, 7–15 wt% MgO; Fig. 3a), with most samples exhibiting low FeO*/MgO ratios (<1.0), in equilibrium with mantle peridotites (Fig. 3a). The major element compositions of these MIs were similar to the whole-rock compositions of the ankaramites from the Kibblewhite Volcano, although the MIs from the magnesian andesites tended to show lower CaO and higher Al_2O_3 contents than those from the ankaramites at similar Mg# values (Fig. 3b). Moreover, the major elemental variations of the Kermadec arc magmas can be explained by fractionating olivine + clinopyroxene (at SiO_2 of <52 wt% and Mg# > 40) and clinopyroxene + plagioclase + magnetite (at SiO_2 > 52 wt% and Mg# < 40) from the Kibblewhite MIs (Fig. 3b). This suggests that these MIs could be parent melts and produce the magmatic variations observed in the Kermadec arc.

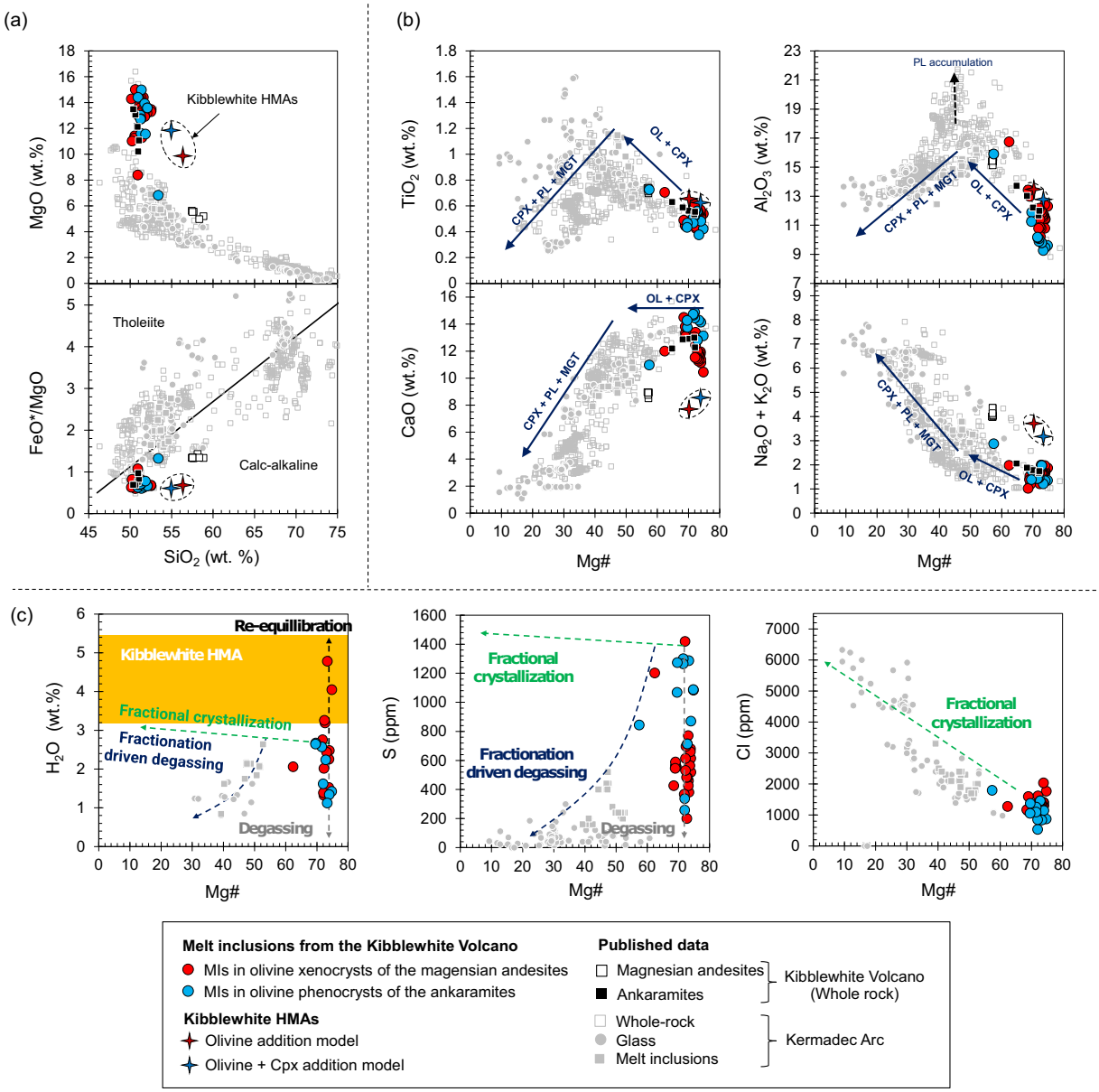

Fig. 3. Major and volatile element variations of the olivine-hosted melt inclusions. (a) Variations of MgO and FeO*/MgO ratio versus SiO_2 contents. The discrimination boundary line in the FeO*/MgO-SiO_2 diagram is from Miyashiro (1974). (b) Variations of TiO_2, Al_2O_3, CaO, and total alkaline ($Na_2O + K_2O$) contents versus Mg# (=100 Mg/[Mg + Fe]). Red and blue crosses indicate the Kibblewhite HMAs (Hirai et al., 2023). The filled and open black squares are whole-rock compositions of the ankaramites and magnesian andesites from the Kibblewhite Volcano (Hirai et al., 2023). Open gray squares are published whole-rock compositions for volcanic rocks from the Kermadec arc front (Barker et al., 2013; Ewart et al., 1994; Gamble et al., 1996, 1997, Gamble et al., 1993; Haase et al., 2002; Timm et al., 2016, Timm et al., 2014; Turner et al., 1997; Wright et al., 2006). Gray circles and squares are published data for glasses and MIs from the Kermadec arc lavas (Barker et al., 2013; Haase et al., 2006; Wysoczanski et al., 2012). (c) Variations of volatile elements (H_2O, S, Cl) in the MIs. Water contents of MIs in magnesian andesites tend to be higher (~5 wt% H_2O) than those in ankaramite (~3 wt% H_2O), which may result from re-equilibration with host magmas. (For interpretation of the references to colour in this figure legend, the reader is referred to the web version of this article.)

4.2.2. Volatile elements

Volatile (H_2O, S, and Cl) contents of the MIs are shown in Fig. 3c. MIs showed variable H_2O contents even at similar Mg#, whereas MIs from the magnesian andesites tended to contain higher water contents (1.3–4.8 wt% H_2O) than those obtained from the ankaramites (1.1–2.7 wt% H_2O). Sulfur contents of the MIs also varied (200–1430 ppm S), suggesting that a variable degree of degassing occurred in the melts prior to entrapment. The MIs contained relatively little Cl (510–2050 ppm) compared to other Kermadec arc magmas. Low Cl contents in MIs suggest that they are plausible candidates for representing primary melts of the Kermadec arc, as Cl is incompatible with olivine. No CO_2-attributed peak was detected in the FTIR spectra of the analyzed MIs, suggesting that any CO_2 was degassed from the melts before entrapment or lost into shrinkage bubbles during post-entrapment crystallization (Wallace et al., 2015). The latter is consistent with the common occurrence of shrinkage bubbles in these MIs, even after homogenization (Fig. S3b).

4.2.3. Trace elements

On the diagram of incompatible trace element variation (Fig. 4a), normalized to normal-type mid-ocean ridge basalt (N-MORB: Sun and McDonough, 1989), all MIs show "arc signatures," such as depletion of high field strength elements (HFSEs: Zr, Nb, Ta, and Hf) compared to heavy rare earth elements (HREEs: Ho, Er, Yb, and Lu) and the peaks associated with large-ion lithophile elements (LILEs: Rb, Sr, Ba, U, Th, and Pb), consistent with other Kermadec arc magmas (e.g., Hirai et al., 2023; Timm et al., 2014). The MIs from the ankaramites showed patterns similar to those of the host rocks, whereas MIs from the magnesian andesites exhibited different patterns to those of the host rocks, indicating a large degree of HFSE depletion (Fig. 4a).

On the diagram of REE variation (Fig. 4b) normalized to C1-chondrite (McDonough and Sun, 1995), MIs from the ankaramites showed REE patterns ranging from almost flat to light rare-earth element (LREE)-depleted. MIs from the ankaramites had similar REE compositions to those of the host rocks but were different from those of the magnesian andesite MIs, showing a more LREE-depleted pattern. MIs from the magnesian andesites showed REE patterns ranging from nearly flat to slightly LREE-enriched and average compositions with a similar slope to those of the host rocks but displaced to lower values.

Fig. 4c shows the variations in selected trace element ratios (Nb/Yb, Ba/Nb, La/Yb, and Nb/Zr) that are not changed significantly by fractionation of the observed phenocrysts (olivine, clinopyroxene, and plagioclase) in the host rocks. Ankaramite MIs showed trace element ratios consistent with those of the host rock, but MIs from the magnesian andesites showed low Nb/Yb values (0.30–0.63) that were inconsistent with those of the host rock (Nb/Yb = 0.80). In addition, MIs from the

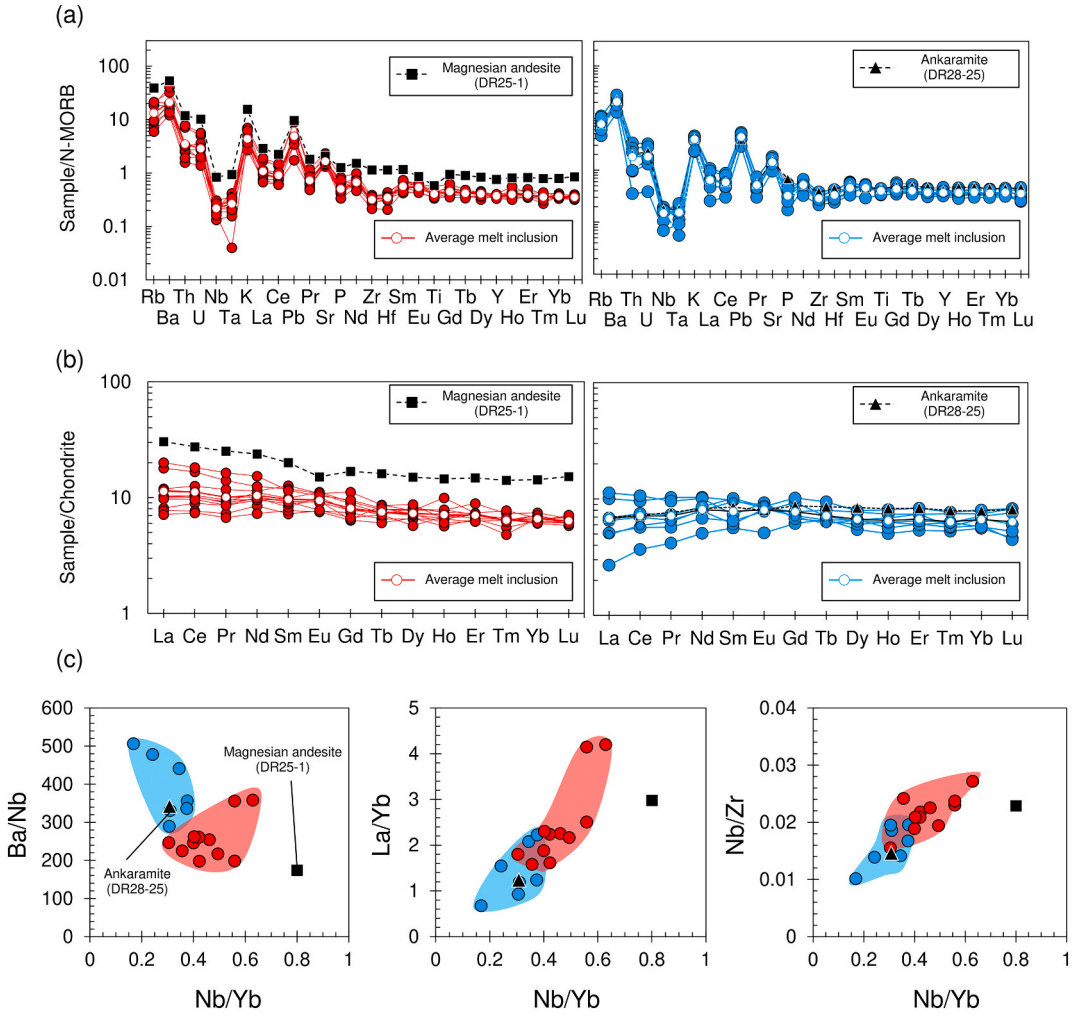

Fig. 4. Trace element variations of olivine-hosted MIs from the magnesian andesites (red) and ankaramites (blue). (a) Normal-type mid-ocean ridge basalt (N-MORB; Sun and McDonough, 1989)-normalized trace element patterns. (b) C1 chondrite (McDonough and Sun, 1995)-normalized rare earth element patterns. (c) Variations of Bz/Nb, La/Yb, and Nb/Zr versus Nb/Yb. Black square and triangle indicate whole-rock compositions of magnesian andesite (DR25–1) and ankaramite (DR28–25) from the Kibblewhite Volcano (Hirai et al., 2023). (For interpretation of the references to colour in this figure legend, the reader is referred to the web version of this article.)

magnesian andesites were characterized by higher Nb/Yb, La/Yb, and Nb/Zr ratios and lower Ba/Nb ratios than those from the ankaramites.

4.2.4. CaO/Al_2O_3 in the melt inclusions

Even if we focus on inclusions in host olivines with Fo >90, MIs from the Kibblewhite ankaramites have CaO/Al_2O_3 ratios of 1.31–1.54, even higher values than those of the magnesian andesites and oceanic arc ankaramites. MIs from the magnesian andesites show variable CaO/Al_2O_3 ratios of 0.85–1.23, which range from plausible values for peridotite-derived melts (CaO/Al_2O_3 < 1.0) to those for oceanic arc ankaramites. Notably, the correction for post-entrapment crystallization, which iteratively adds equilibrium olivines to the MIs, does not affect the CaO/Al_2O_3 ratios of the MIs because of the low CaO and Al_2O_3 concentrations in the olivine. Thus, the variable CaO/Al_2O_3 ratio in these MIs is an original characteristic.

Moreover, we observed an unexpected correlation between CaO/Al_2O_3 ratios in the MIs and the NiO content of the host olivines. Fig. 5 shows that CaO/Al_2O_3 in the MIs from the magnesian andesites is negatively correlated with the NiO content in the host olivines. In other words, MIs with high CaO/Al_2O_3 ratios were hosted in olivines with low NiO contents. MIs from the ankaramites have uniformly high CaO/Al_2O_3 ratios but are hosted in olivines with uniformly low NiO contents. This suggests that the variation in CaO/Al_2O_3 ratios of the MIs could be due to any process that additionally causes a simultaneous change in the Ni content of the melt. Additionally, some major and compatible trace elements were correlated with CaO/Al_2O_3 (Fig. 6). CaO/Al_2O_3 ratios in the MIs from the magnesian andesites were positively correlated with SiO_2, CaO, Sc, and Cr and negatively correlated with Al_2O_3 and Ni. MgO and Mg# also exhibited slightly negative correlations with CaO/Al_2O_3. Notably, the melt inclusion with the lowest CaO/Al_2O_3 ratio has a major element composition consistent with peridotite melts produced experimentally in a laboratory (Kushiro, 1996). These observed variations between CaO/Al_2O_3 ratios and major and trace elements suggest that the composition of the Kibblewhite MIs has changed from peridotite-derived melts to ankaramite melts.

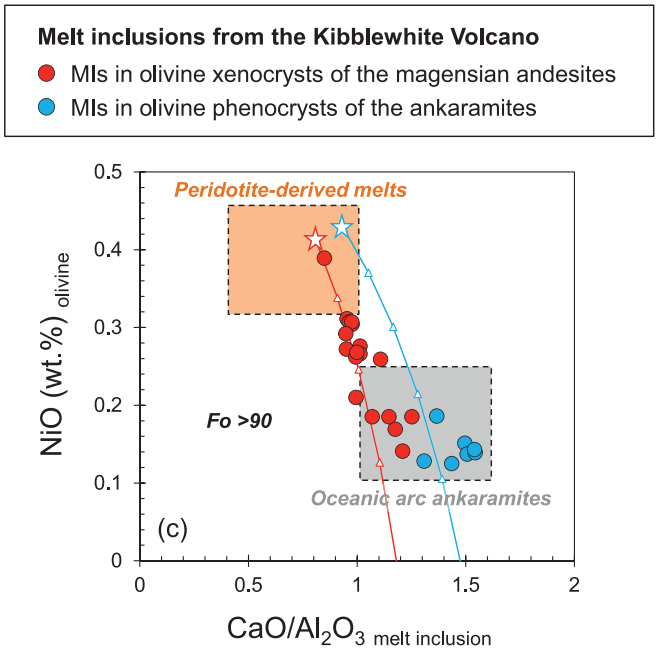

Fig. 5. Correlation between CaO/Al_2O_3 in the MIs and NiO content in their host olivines (shown only in samples with Fo >90). Orange and gray fields represent the range of mantle-derived melt (CaO/Al_2O_3 < 1.0; NiO >0.2 wt%) and oceanic arc ankaramites (CaO/Al_2O_3 > 1.0; NiO <0.2 wt%), respectively. The red and blue lines with open triangles indicate the estimated compositional change in melts during assimilation-fractional crystallization (AFC) models shown in Table S4. Open red and blue stars represent the initial melt compositions from Kushiro (1996), used for the AFC models (see text for details). (For interpretation of the references to colour in this figure legend, the reader is referred to the web version of this article.)

5. Discussion

5.1. Do MIs represent primary melts occurring in the Kibblewhite region?

Most Kibblewhite MIs were hosted in forsteritic olivines ($Fo_{90–92}$) and thus show high Mg# that can be in equilibrium with mantle peridotites after correction for post-entrapment crystallization. Since such high-Fo olivines must have crystallized from primary melts generated by mantle melting, these MIs are likely to reflect the parental melt compositions of the host rocks. Indeed, the MIs from the ankaramites show major and trace element compositions consistent with those of the host rocks (Figs. 3 and 4), indicating that they represent the host magma composition. Although the MIs from the ankaramites exhibited a high degree of trace element variation compared with the host rock, their average composition matched that of the host rock (Fig. 4). This may indicate that the melt was locally heterogeneous but that the whole-rock composition reflected the average (Kent, 2008). Thus, the MIs from the ankaramites are plausible parental melts of the ankaramites, and no reason exists to suspect that the ankaramites of the Kibblewhite Volcano resulted from the accumulation of olivine and clinopyroxene crystals.

However, the MIs hosted in the olivine xenocrysts of the magnesian andesites may not represent the parental melts of the magnesian andesites. Hirai et al. (2023) estimated the primary melt compositions of the magnesian andesites, termed “Kibblewhite high-magnesian andesites (HMAs),” using olivine-addition models. The major element compositions of the MIs from the magnesian andesites are not consistent with those of the Kibblewhite HMAs but are instead similar to those of the ankaramites (Fig. 3a, b). The incompatible trace element patterns of the MIs also differ from those of the host magnesian andesites, which showed greater HFSE depletion against HREEs (Fig. 4c). The Nb/Yb ratios in the MIs of the magnesian andesites were also lower than those in the host rock (Fig. 4c). Therefore, we can conclude that the MIs hosted in the olivine xenocrysts of the magnesian andesites are not parental melts of the magnesian andesites but primitive basaltic melts that could have been produced before the occurrence of the magnesian andesites.

Instead, the large variation in H_2O in the MIs from the magnesian andesites may reflect the water content of the host magmas. Recent studies have revealed that water content in melt inclusions can fully re-equilibrate with the host magma within hours via H^+ diffusion through olivine (Gaetani et al., 2012; Lloyd et al., 2013; Portnyagin et al., 2019). The olivine xenocrysts in the magnesian andesites remained inside the host magmas for at least 5 days (see Section 2), suggesting that the water contents of the MIs reached re-equilibration with the host magmas. Hirai et al. (2023) estimated that the Kibblewhite HMAs were directly produced by melting mantle peridotite at 1.1–1.3 GPa with 3.2–5.5 wt% H_2O; this is consistent with H_2O contents in the MIs from the magnesian andesites (Fig. 3c). Thus, the original water content in these MIs should have been lost, but the MIs in olivine xenocrysts of the magnesian andesites may reflect the water contents in their host magmas.

The difference in trace element characteristics between the MIs from the ankaramites and magnesian andesites (Fig. 4) may also reflect different conditions in the mantle wedge. The systematic differences in trace element compositions between the MIs can be attributed to trench-perpendicular variation. Fig. 7 shows the trench-perpendicular variations in $^{87}Sr/^{86}Sr$, $^{206}Pb/^{204}Pb$, Ba/Nb, Nb/Zr, and Nb/Yb in the volcanic rocks and MIs collected from the Kibblewhite region. The $^{87}Sr/^{86}Sr$, $^{206}Pb/^{204}Pb$, and Ba/Nb ratios in the volcanic rocks from the Kibblewhite region decrease with increasing distance from the trench, whereas the Nb/Zr and Nb/Yb ratios increase. LILEs (Sr, Pb, Ba) are easily lost to slab-derived fluids within a wide range of temperatures (700–1000 °C), but HFSEs (such as Nb) are not (Kessel et al., 2005). The

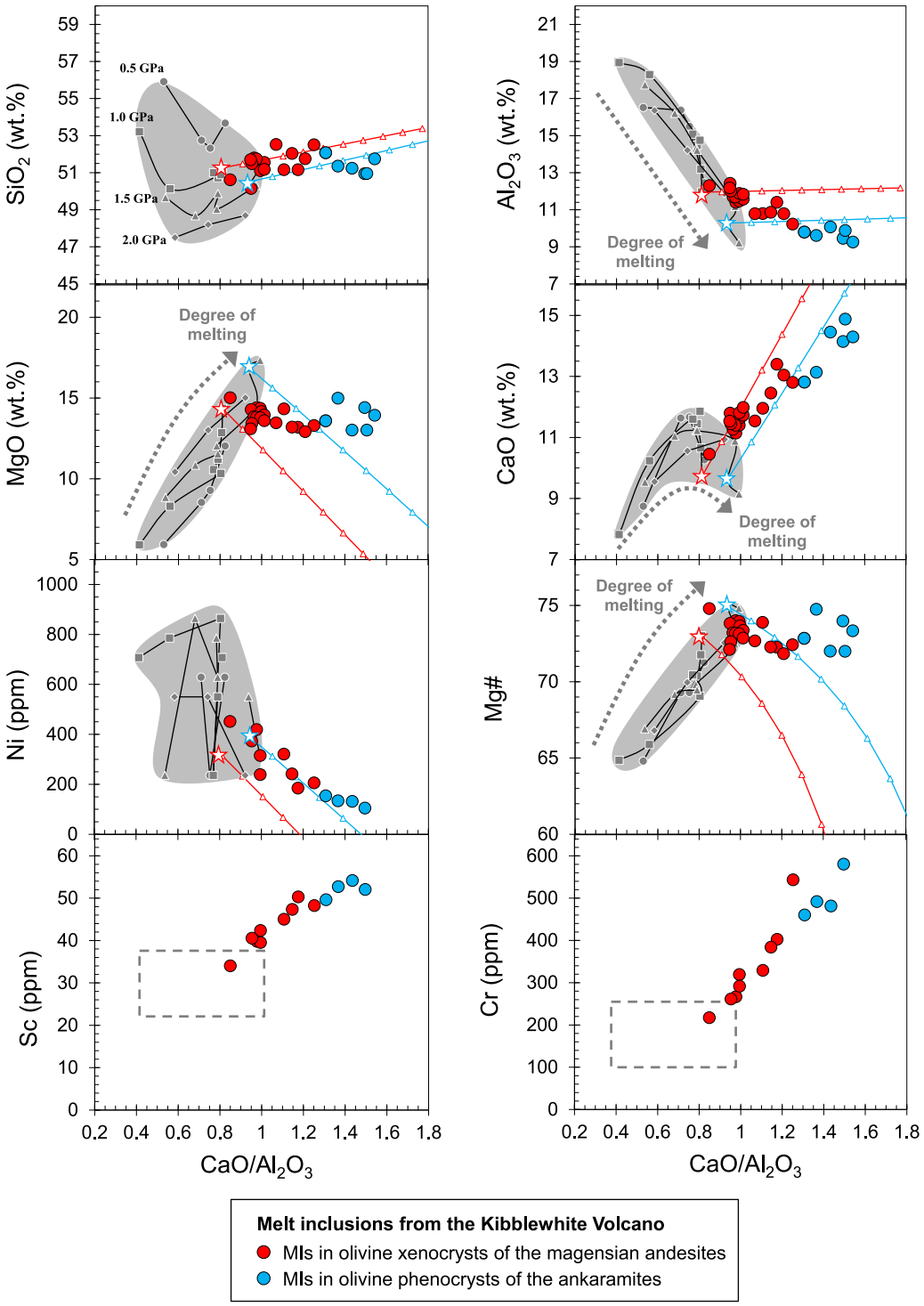

Fig. 6. Correlations between CaO/Al_2O_3 and major elements in the MIs (shown only for Fo >90 samples). Black lines with gray symbols indicate the compositions of melt obtained from dry melting experiment of lherzolite PHN1611 at 0.5 to 2.0 GPa (Kushiro, 1996). The red and blue lines with open triangles indicate the estimated compositional change in melts during assimilation-fractional crystallization (AFC) models shown in Table S4. Open red and blue stars represent the initial melt compositions from Kushiro (1996), used for the AFC models (see text for details). (For interpretation of the references to colour in this figure legend, the reader is referred to the web version of this article.)

contribution of slab-derived components to the depleted mantle beneath the Kermadec arc should have increased the Sr and Pb isotope ratios of the melts (Timm et al., 2014). Thus, the decrease in the Sr and Pb isotope ratios and Ba/Nb values may represent a decrease in the contribution of the slab-derived components to the source from the trench side to the rear-arc side. However, the increase in the Nb/Zr and Nb/Yb ratios, which are less affected by slab-derived components, may indicate a decrease in the degree of source mantle depletion towards the rear-arc side. This is because the Nb/Zr ratio in the melt hardly changes with the degree of partial melting of the source mantle (Langmuir et al., 2006). Generally, the mantle will produce more melt and become depleted if more slab-derived water is added. Thus, the increase in the Nb/Zr and Nb/Yb ratios may represent a decrease in the degree of source mantle depletion from the trench side to the rear arc side, which is

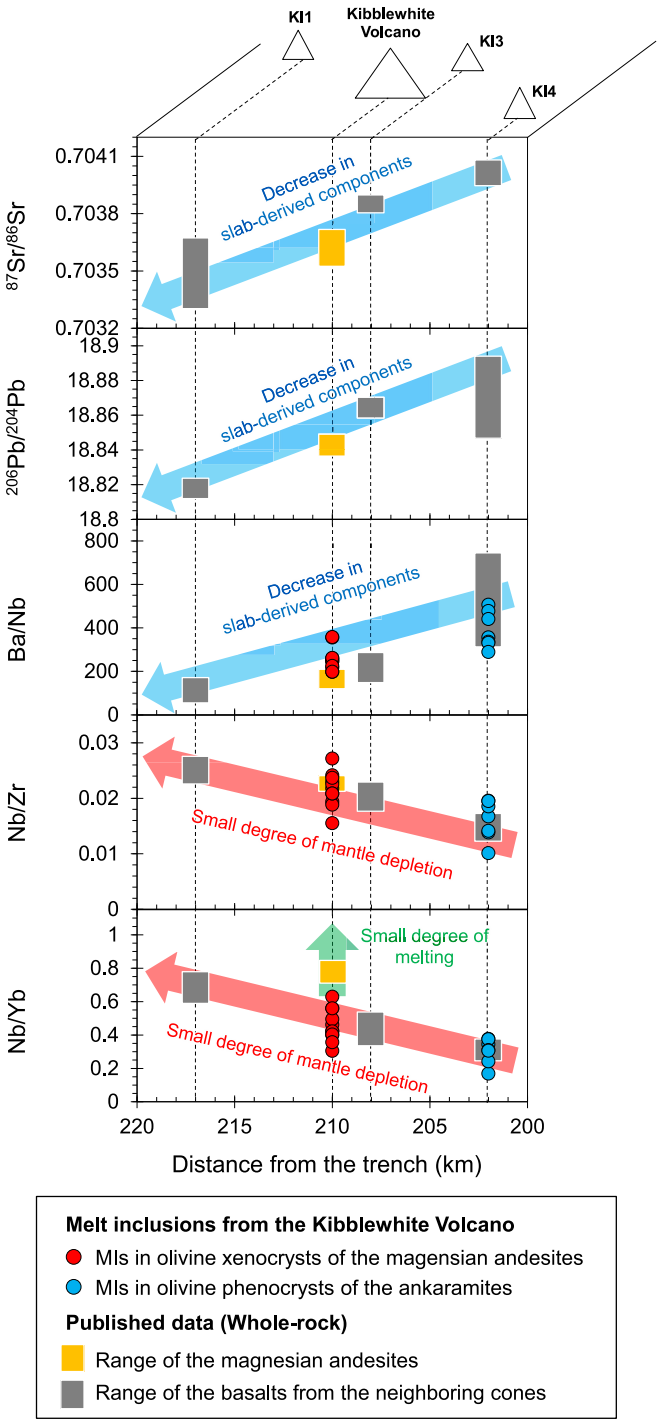

Fig. 7. Trench-perpendicular variations of $^{87}Sr/^{86}Sr$, $^{206}Pb/^{204}Pb$, Ba/Nb, Nb/Zr, and Nb/Yb in volcanic rocks and melt inclusions collected from the Kibblewhite region. The approximate distances from the trench for each volcanic edifice were measured on Google Maps.

consistent with the abovementioned trench-perpendicular variation of the slab-derived components. The trace element variations of the studied MIs are consistent with the trends formed by basalts from neighboring cones (Fig. 7), indicating that they also reflect trench-perpendicular variations in the source mantle.

However, noting that the magnesian andesites have higher Nb/Yb ratios than the MIs hosted in their olivine xenocrysts is important, even though they have similar Nb/Zr ratios (Fig. 7). Since Nb/Yb in the melt is more sensitive than Nb/Zr to changes in the degree of melting, this can be attributed to the magnesian andesites being generated by a lower degree of melting than the MIs. The lower degree of melting in the magnesian andesites is closely related to their origin, as discussed below.

In summary, MIs from the ankaramites have major and trace element characteristics consistent with those of the host rock, indicating that they represent a primary magma component in the Kibblewhite region. The MIs from the magnesian andesites were hosted in olivine xenocrysts and did not represent the host magma. Instead, they may represent primary basaltic melts generated before the occurrence of the magnesian andesites.

5.2. Origin of the ankaramitic Kibblewhite melt inclusions

5.2.1. Grain-scale modification

A primary concern is whether these chemical variations in the MIs were caused by grain-scale processes and, therefore, do not reflect the primary magmatic variation. Danyushevsky et al. (2004) reported primitive MIs with anomalous compositions and proposed that they reflected localized grain-scale assimilation processes within the crust. The correlation between CaO/Al_2O_3 and Ni in the MIs studied here may be explained by the assimilation of clinopyroxene into the melts.

This model may explain the compositional variation of the MIs but cannot account for the significant volume of the ankaramitic magmas. As discussed above, the major elemental composition of the MIs from the ankaramites is consistent with the whole-rock composition of the host rock, and large quantities of ankaramites have been recovered from neighboring cones as lava blocks. Other oceanic arc ankaramites have been observed as lava flows or pillow lavas (Barsdell, 1988; Barsdell and Berry, 1990; Tamura et al., 2014). These ankaramitic magmas clearly produced a significant amount of lava, which cannot be explained by grain-scale processes. Thus, we believe that ankaramite magma must form one of the main magma components in oceanic arcs and that the high CaO content and high CaO/Al_2O_3 in these MIs need not be ascribed to grain-scale processes within the crust.

5.2.2. Melting of lower crustal wehrlites

Primitive basaltic rocks or MIs with $CaO/Al_2O_3 > 1.0$ have previously been known as "ultra-calcic melts" (Schiano et al., 2000) and can be divided into nepheline-normative and hypersthene-normative suites based on the degree of silica undersaturation (Fig. 8a). Through multiple saturation experiments, Médard et al. (2004) concluded that the nepheline-normative suites are derived from lower crustal conditions (0.2 GPa, 1220 °C). Médard et al. (2006) also showed that the melting of amphibole-bearing wehrlite reproduces the major element compositions of nepheline-normative ultra-calcic melts (Fig. 8a). Based on these experimental constraints, Sorbadere et al. (2011, 2013) concluded that amphibole-bearing wehrlite at the lower-crust or the uppermost mantle plays a key role in generating the nepheline-normative ultra-calcic melts in island-arc volcanoes. Alternatively, Portnyagin et al. (2019) proposed that nepheline-normative ultra-calcic MIs, often observed in sub-areal arc settings, are generated by the coupled loss of H_2O and SiO_2 from the initially trapped hypersthene-normative melts (Fig. 8a). Nevertheless, a consensus exists that nepheline-normative ultra-calcic melts are not representative of mantle-derived primary magmas.

When the Kibblewhite MIs are projected onto the Di-Plag-Qz space (from the Ol apex) on the "basalt tetrahedron" after Falloon and Green (1988), they plot as hypersthene-normative, similar to the oceanic arc ankaramites (Fig. 8a). This strongly suggests that the CaO/Al_2O_3 ratios in the Kibblewhite MIs did not result from the melting of lower crustal wehrlites. Therefore, we believe that the contribution of lower crustal wehrlite to the Kibblewhite MIs was either absent or minimal.

5.2.3. Contribution of pyroxenite to the source mantle

A recent study emphasized the contribution of pyroxenite-derived melts to the origin of subduction zone magmas (Bowman and Ducea, 2023). Since the addition of pyroxene components could explain the

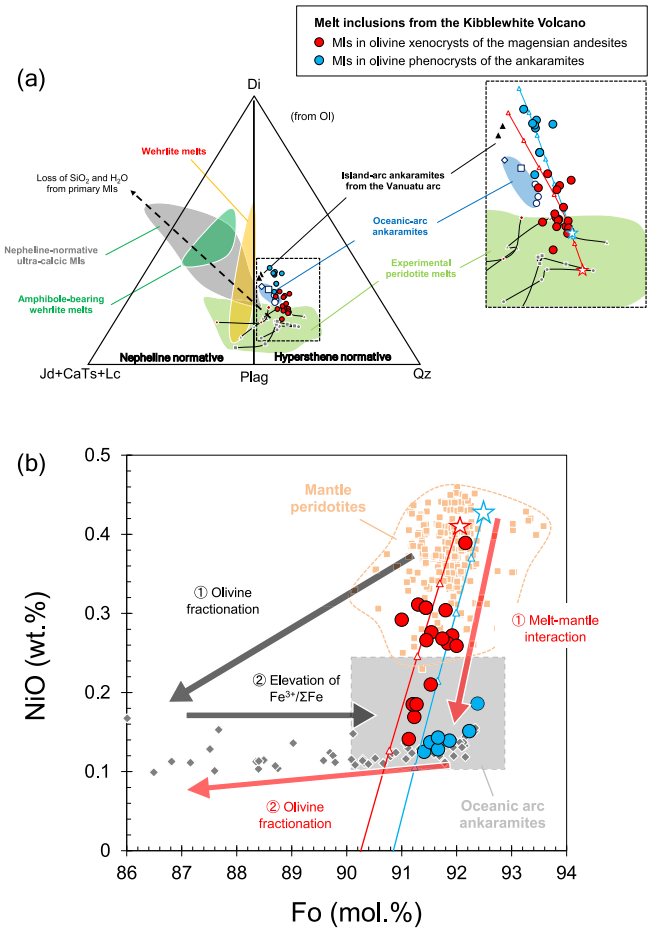

Fig. 8. (a) Normative compositions of the olivine-hosted MIs (shown only for host olivines with Fo >90) and oceanic arc ankaramites, projected from Ol onto the Di-Jd + CaTs+Lc-Qz face of the "basalt tetrahedron" after Falloon and Green (1988). The field of the wehrlite melts at 1.0 to 2.0 GPa is after Pickering-Witter and Johnston (2000) and Kogiso and Hirschmann (2001). The field of the amphibole-bearing wehrlite melts at 1.0 GPa is after Médard et al. (2006). Data sources for the nepheline-normative ultra-calcic MIs are from Kamenetsky et al. (1995, 2017), Della-Pasqua and Varne (1997), Portnyagin et al. (2005), Elburg et al. (2007), Sorbadere et al. (2011), and Métrich and Deloule (2014). The broken arrow indicates the presumed compositional change of melt inclusions during a coupled loss of SiO_2 and H_2O from the inclusions (Portnyagin et al., 2019). Black lines with gray symbols indicate the melt compositions from the dry melting experiment of lherzolite PHN1611 at 0.5 to 2.0 GPa (Kushiro, 1996). The red and blue lines with open triangles indicate the compositional change in melts estimated by the assimilation-fractional crystallization (AFC) models shown in Table S4. (b) Two models that produce low NiO olivine with high Fo content. The dark gray arrows indicate the hypothesis that the primary melt crystallized olivine (trend 1), and then the $Fe^{3+}/\Sigma Fe$ ratio in the melt is increased by degassing, increasing Fo content in olivine (trend 2). The red arrows indicate the hypothesis that the Ni content in the melt decreases but the Mg# in the melt remains almost constant due to the melt-mantle interaction (trend 1), and then the interacted melt crystallized olivine with low NiO content (trend 2). Open red and blue stars represent the olivine compositions in equilibrium with the initial melt compositions used for the AFC models. The red and blue lines with open triangles indicate the estimated compositional change of the olivine in equilibrium with the melts from the AFC models. (For interpretation of the references to colour in this figure legend, the reader is referred to the web version of this article.)

high CaO/Al_2O_3 ratio in oceanic arc ankaramites, this model should be considered. However, we believe that this model is not a good fit for the origin of Kibblewhite MIs because it cannot explain the low Ni content. Pyroxenite (or a hybrid of pyroxene and peridotite)-derived melts have a higher Ni content than that derived from ordinary mantle peridotite (Nishizawa et al., 2017; Sobolev et al., 2005; Straub et al., 2011, Straub et al., 2008). This is because the rock/melt distribution coefficient of Ni decreases as the proportion of olivine in the whole rock composition decreases. This model, therefore, conflicts with the low Ni content of Kibblewhite ankaramites. Furthermore, the degree of contribution of pyroxenite-derived melts is proportional to the crustal thickness in subduction zones (Bowman and Ducea, 2023). As the Kermadec arc has some of the thinnest crust worldwide, a significant contribution of pyroxenite-derived melts to the Kibblewhite MIs is unlikely.

5.2.4. *Melting of the carbonated mantle and degassing of CO_2*

Multiple saturation experiments using the hypersthene-normative ankaramite from the western Epi Volcano in the Vanuatu arc revealed that they are saturated with olivine + clinopyroxene or only clinopyroxene at mantle conditions (1.2–2.0 GPa, 1300–1400 °C; Médard et al., 2004; Schmidt et al., 2004). This suggests that the western Epi ankaramites are not in equilibrium with ordinary mantle peridotite, consisting of olivine + orthopyroxene ± clinopyroxene. Schmidt et al. (2004) proposed that the western Epi ankaramites experienced olivine fractionation from primary melts that initially had high CaO/Al_2O_3. For the generation of such initially high-CaO/Al_2O_3 melts, Green et al. (2004) emphasized the importance of a carbonation reaction between mantle wedge peridotites and CO_2-rich dolomitic fluids from the subducting slab. This reaction may have formed carbonate-bearing peridotite in the mantle wedge and finally produced melts with high CaO/Al_2O_3. Green et al. (2004) suggested that the low olivine NiO content in the ankaramites could be explained by the elevation of Fe^{3+}/Fe^{total} in the melts due to the degassing of CO_2-rich fluids from the melts. This is because the elevation of Fe^{3+}/Fe^{total} may increase the Fo content in the olivine phenocrysts but not the NiO content.

However, this model does not fully explain the origin of the CaO/Al_2O_3 variation in Kibblewhite MIs for the following reasons: First, this model requires a primary melt with an initially high CaO/Al_2O_3 ratio because olivine fractionation does not significantly change CaO/Al_2O_3 in the melt. However, the CaO/Al_2O_3 ratio in the Kibblewhite MIs varied consistently from ordinary peridotite-derived melts to ankaramitic melts (Fig. 5). Thus, these MIs suggest that CaO/Al_2O_3 in the primary melt was low, as in the peridotite-derived melts, but then increased subsequently through other processes. Second, this model cannot explain the NiO variations in the host olivine of the MIs studied here. If the low NiO contents of the olivines in the ankaramites were caused by the fractionation of olivine from primary magma and elevation of $Fe^{3+}/\Sigma Fe$ in the magma by subsequent degassing, the NiO contents in the fractionated olivines should decrease with Fo content (as shown by the dark gray arrows in Fig. 8). Thus, this model cannot account for vertical variations in the host olivine on the Fo-NiO diagram. For these reasons, we infer that the contribution of CO_2-rich fluids from the subducting slab is not an essential cause of the compositional variations in the Kibblewhite MIs. Instead, we show in the next section that melt-mantle interaction can plausibly explain the vertical variation in the host olivine on the Fo-NiO diagram (red arrows in Fig. 8).

5.2.5. *Melt-mantle interaction*

Kelemen (1990) showed that primary basaltic melts, produced at high pressure, interact with the surrounding mantle during ascent. At shallower depths, ascending basaltic melts are saturated with olivine but unsaturated with pyroxenes; they precipitate olivine and assimilate pyroxenes from the surrounding lithospheric mantle. During this assimilation-fractional crystallization (AFC) process, the Mg# of the ascending basaltic melts remains constant because it is buffered by Fe—Mg exchange with the assimilated pyroxenes (Kelemen, 1990). Based on this AFC model, Tamura et al. (2019a) proposed that the low NiO contents of olivines in ankaramites from the Nishinoshima Volcano were caused by melt-mantle interactions during the ascent of the primary basaltic melts.

We believe that this model can explain not only the low NiO content in olivine but also the high CaO/Al_2O_3 ratio in the MIs studied here. Kelemen et al. (1992) proposed that such melt–mantle interactions ultimately produce a harzburgite residue at the uppermost mantle. Due to the melt-mantle interaction, the ascending basaltic melt gradually becomes saturated with orthopyroxene as the temperature decreases. If the melt continues to percolate through the lherzolite mantle after orthopyroxene saturation, it produces harzburgite via a melt-rock reaction with lherzolite and hence becomes saturated with clinopyroxene. Until the melt reaches clinopyroxene saturation, it assimilates clinopyroxene and precipitates olivine and orthopyroxene as it ascends through the lherzolite mantle. If the melt erupts before clinopyroxene saturation is reached, it should be rich in clinopyroxene (diopside) component. The high CaO/Al_2O_3 and major and compatible trace element variations in the MIs studied here may be explained by the addition of a clinopyroxene (diopside) component to the peridotite-derived melts (Figs. 1 and 6), suggesting that these variations could be produced by melt-mantle interaction.

To simulate the compositional change of basaltic melts during the melt-mantle interaction, we conducted a simple mass-balance calculation for the AFC process. In this model, two experimental peridotite melts from Kushiro (1996), which were produced at different pressures (1.0 and 1.5 GPa) and degrees of melting (29% and 36%), were assumed as the initial melts. These initial melts were selected for their compositional similarity to the MIs studied here and are thus not representative of the actual melting pressure or degree of melting. The assimilated to crystallized mass (Ma/Mc) ratio was assumed to be 0.97 after Kelemen et al. (1992). The olivine to orthopyroxene ratio in the fractionated phase was assumed to be 0.5. Since the chemical composition of the mineral phases in the Kermadec arc mantle peridotite is still unknown, forearc peridotites from the Tonga arc (Birner et al., 2017) were used for the calculation. The modeling results are listed in Table S4.

The modeling results indicate that the initial melts increase in CaO and CaO/Al_2O_3 and decrease in MgO, Ni, and Mg#, qualitatively reproducing the correlation between CaO/Al_2O_3 and major elements in the Kibblewhite MIs (Fig. 6). The differences between the two initial melts in the model suggest that the compositional differences between the MIs from the ankaramites and magnesian andesites may be derived from differences in the melting pressure and degree of melting of the initial melts. The variations in NiO in the host olivines, estimated from the olivine-melt Ni partition coefficient, indicate that this model can also reproduce the vertical variation in the host olivines seen on the Fo-NiO diagram (Fig. 8). Furthermore, this AFC model can also explain the unexpected correlation between CaO/Al_2O_3 in the MIs and NiO in the host olivines (Fig. 5). Therefore, we propose that the abnormal variations between the CaO/Al_2O_3 of the Kibblewhite MIs and NiO of the host olivines resulted from the interaction between the ascending primary

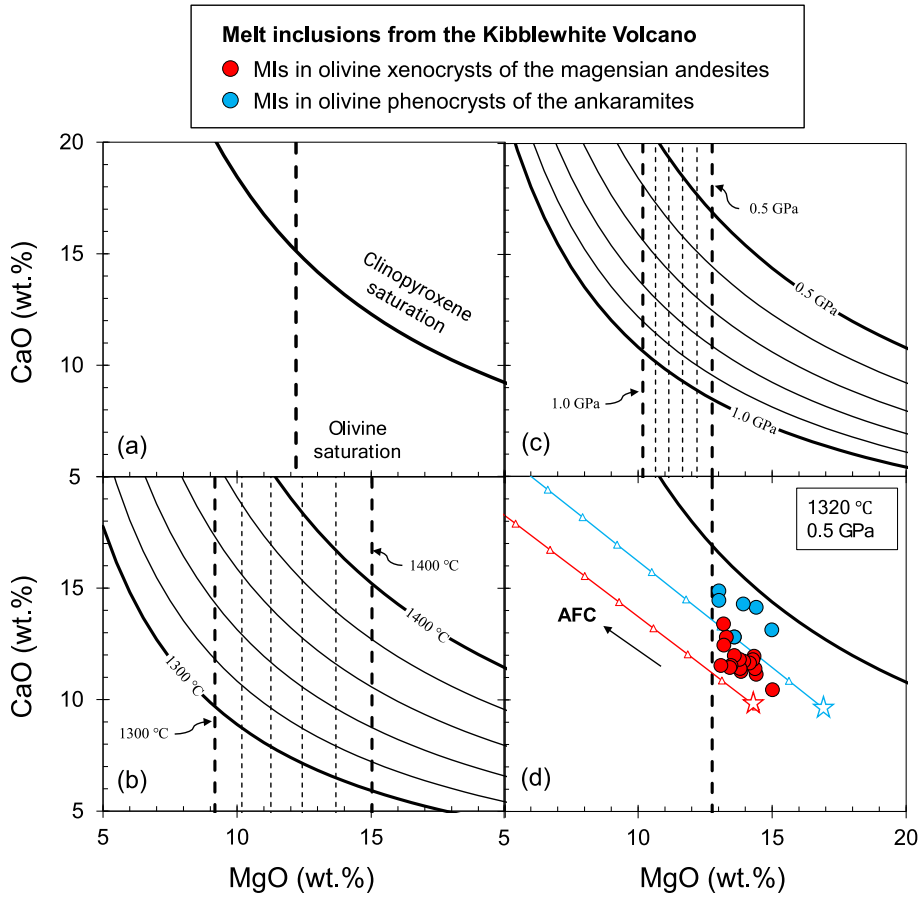

Fig. 9. MgO–CaO composition regime illustrating the saturation status of olivine and clinopyroxene. (a) Dashed vertical line represents the melt composition at olivine saturation, after Chen and Zhang (2008). Curved line represents the melt composition at clinopyroxene saturation after Chen and Zhang (2009). (b) Temperature dependence of the saturation curves at 1 GPa. (c) Pressure dependence of the saturation curves at 1320 °C. (d) Application of the olivine and clinopyroxene saturation models to the MIs studied here. If these basaltic melts are at 1320 °C and under pressure conditions of the uppermost mantle of the Kermadec arc (0.5 GPa), they will be over-saturated with olivine and under-saturated with clinopyroxene. Thus, the melts will fractionate olivine and assimilate clinopyroxene from the surrounding mantle. The red and blue lines with open triangles indicate the compositional change in melts estimated by AFC models shown in Table S4. Open red and blue stars represent the initial melt compositions from Kushiro (1996), used for the AFC models (see text for details). (For interpretation of the references to colour in this figure legend, the reader is referred to the web version of this article.)

basaltic melts and surrounding mantle peridotites in the mantle wedge.

However, a question remains as to whether the initial basaltic melts become ankaramitic before reaching clinopyroxene saturation. We infer that the thin crust of the Kermadec arc plays an important role in the generation of ankaramitic melts. Chen and Zhang (2009) proposed that the olivine and clinopyroxene saturation of a basaltic melt is approximately determined by the MgO and CaO contents of the melt (Fig. 9a). The MgO and CaO contents of the melt at clinopyroxene saturation are positively correlated with the temperature (Fig. 9b); therefore, as the temperature decreases at constant pressure, the melt will become saturated with clinopyroxene. Conversely, MgO and CaO contents at clinopyroxene saturation are negatively correlated with pressure (Fig. 9c); thus, as the pressure decreases at a constant temperature, the melt will not reach clinopyroxene saturation. When this model is applied to the Kibblewhite MIs, assuming a temperature of 1320 °C and low-pressure conditions of 0.5 GPa, they are still not saturated with clinopyroxene but are saturated with olivine (Fig. 9d). Hence, the primary basaltic melt will assimilate clinopyroxene and crystallize olivine even under these conditions.

We do not consider this P-T condition to be an overestimation for the following reasons. First, the high Fo contents of the host olivines of the Kibblewhite MIs indicate a high magmatic temperature. The magmatic temperature correlates with the MgO content of the melt (Sugawara, 2000) and, thus, the Fo content of the equilibrium olivine. To examine this more specifically, we estimated the generation conditions of the Kibblewhite MIs using the geothermobarometer described in Mitchell and Grove (2015). For this estimation, we used the composition of sample DR25–3 OLB3_MI1, which has the least influence on melt-mantle interaction, that is, the lowest CaO/Al_2O_3 ratio among the MIs hosted in olivine with Fo > 90. Assuming that the melt contained 3.0 wt% H_2O, based on the actual H_2O content (Fig. 3c), the geothermobarometer suggests that the melt was produced at 1310 °C and 1.6 GPa. The thin crust in this area results in a low-pressure condition in the uppermost mantle wedge of the Kermadec arc. The estimated crust-mantle boundary of the Kermadec arc is ~15 km (Bassett et al., 2016), corresponding to pressures of ~0.5 GPa. Thus, the primary basaltic melts produced at 1.6 GPa, corresponding to a depth of ~50 km, would inevitably interact with the shallower lithospheric mantle before reaching the crust. For these reasons, we believe that this model is plausible for the Kibblewhite region in the Kermadec arc and conclude that it is possible to produce ankaramitic melts using the AFC of ascending basaltic melts in the mantle wedge.

5.3. Implications for the origin of the magnesian andesites

Yogodzinski et al. (1994) noted that high-magnesian andesites from Piip Volcano in the western Aleutian arc have significantly lower CaO/Al_2O_3 ratios than lherzolite-derived melts. They attributed this low CaO/Al_2O_3 ratio in the Piip andesites to a reaction between the primary basaltic melts and harzburgites at low pressures. Using an experimental approach, Wood and Turner (2009) suggested that HMAs from subduction zones were produced by the melting of the harzburgite mantle. The Kibblewhite HMAs are presumed to have low CaO/Al_2O_3 ratios, similar to the other HMAs (Fig. 1a), implying that they are derived from clinopyroxene-poor source mantle.

As summarized in Fig. 10, we propose that melt-mantle interaction produces a "harzburgite passage," which is closely related to the origin of the magnesian andesites, in the mantle wedge beneath the Kibblewhite Volcano. The initial basaltic melts, produced by melting of a deeper part of the mantle wedge, interact with the surrounding mantle

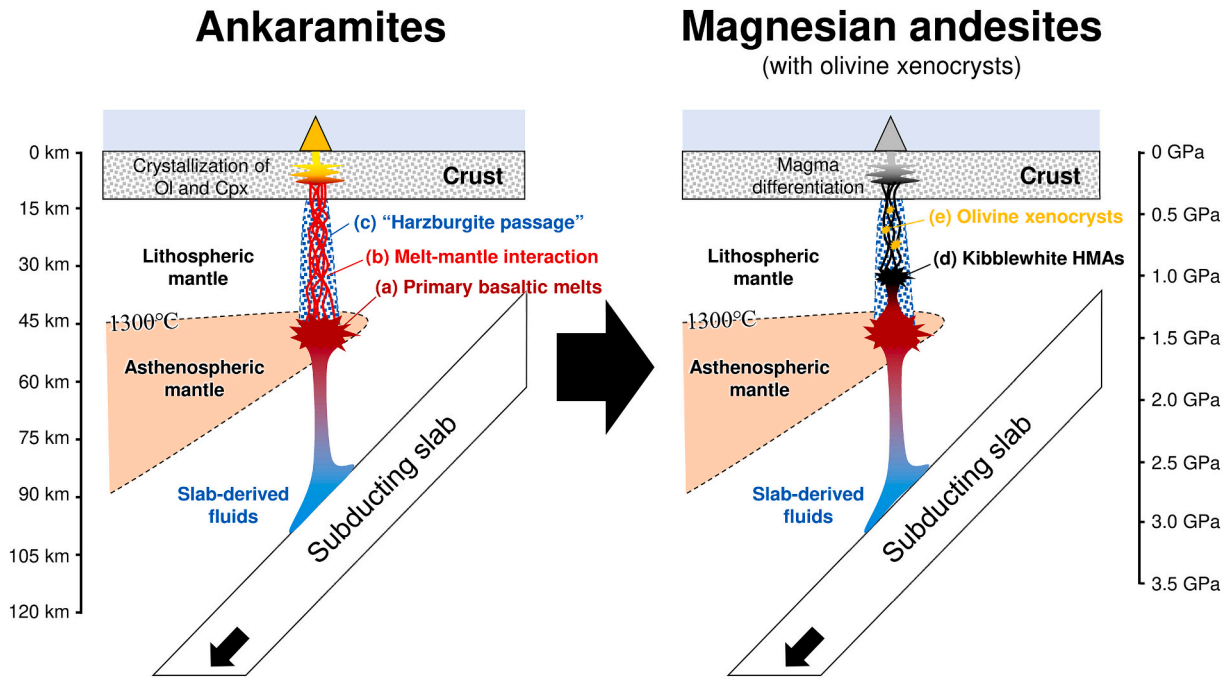

Fig. 10. Schematic illustration showing the origin of the MIs and their relation to magnesian andesites from the Kibblewhite Volcano. (a) Primary basaltic melts are produced in a deeper (>1.5 GPa) and hotter (>1300 °C) part of the mantle wedge by hydrous melting caused by the contribution of slab-derided fluids. (b) Reaction occurs between the ascending primary basaltic melts and the surrounding mantle peridotites due to a decrease in pressure. During the interaction, the melts become rich in CaO/Al_2O_3 and poor in Ni due to assimilation of pyroxenes and fractionation of olivine. Eventually, the melts become saturated with and crystallize orthopyroxene and continue to ascend in the mantle wedge while replacing the surrounding lherzolite with harzburgite. (c) This melt-mantle interaction forms a "harzburgite passage" as a residue in the mantle wedge. The interacted melts emplace in a magma chamber in the crust and crystallize abundant olivine and clinopyroxene, producing ankaramites (olivine-clinopyroxene-rich basalts). (d) Subsequently generated primary basaltic melts pass through and re-equilibrate with the harzburgite passage in a shallower (~1.0 GPa) and colder (~1200 °C) part of the mantle wedge, producing primary andesitic melts (Kibblewhite HMAs). (e) Olivine xenocrysts which were produced during the melt-mantle interaction show variable NiO contents and host MIs with variable CaO/Al_2O_3 and are incorporated into the Kibblewhite HMAs during ascent through the harzburgite passage.

during ascent and convert lherzolite to harzburgite via the assimilation of clinopyroxene and fractionation of olivine and orthopyroxene (Kelemen et al., 1992). If, subsequently, ascending basaltic melts again pass through this harzburgite passage, they interact and re-equilibrate with the surrounding harzburgite under low-pressure and low-temperature conditions. This reaction may have transformed the initial basaltic to andesitic melt while decreasing the magma volume (Kelemen, 1990). This model is consistent with the observation that magnesian andesites contain olivine xenocrysts hosting ankaramitic MIs. These olivine xenocrysts may have precipitated within the lithospheric mantle during the "first" melt-mantle interaction and were subsequently incorporated into the magnesian andesite magmas.

This decrease in magma volume can explain the relatively high Nb/Yb (Fig. 7) and H_2O contents (Fig. 3c) of the magnesian andesites. This is because a decrease in magma volume in the mantle causes a compositional change in the melt, similar to a decrease in partial melting. In addition, because water is incompatible with mantle minerals, even if the initial water content of the basaltic melt is similar to that of the ankaramites (2–3 wt% H_2O), the water content of the produced primary andesitic melt will be higher if the magma volume decreases during the melt-mantle interaction. Therefore, we propose that the magnesian andesites (Kibblewhite HMAs) were produced by the re-equilibration of primary basaltic melts with a refractory harzburgite, which was formed by a previous melt-mantle interaction in the uppermost mantle.

6. Conclusion

This study investigated olivine-hosted MIs from ankaramites and magnesian andesites in the Kibblewhite Volcano in the Kermadec arc. The main conclusions of this study are summarized as follows:

(1) The MIs from the ankaramites have major and trace element characteristics consistent with those of the host rock, indicating that they are a primary magma component in the Kibblewhite region. The MIs from the magnesian andesites are hosted in olivine xenocrysts and thus do not represent the host magma but rather the primary basaltic melts generated before the occurrence of the magnesian andesites.
(2) The CaO/Al_2O_3 and Ni contents in the Kibblewhite MIs can be explained by melt-mantle interaction. If primary basaltic melts interacted with the surrounding mantle during ascent into the mantle wedge, the ascending basaltic melts would have assimilated clinopyroxene and fractionated olivine and orthopyroxene at a constant melt Mg#. Thus, due to this interaction, the melts become rich in CaO/Al_2O_3 and poor in Ni, and a "harzburgite passage" will be formed in the mantle wedge as a residue.
(3) The magnesian andesites are derived through the "harzburgite passage" formed by prior melt-mantle interaction. The thin crust of the Kermadec arc allows hot basaltic melts to re-equilibrate with harzburgite under low-pressure conditions. This re-equilibration produces primary andesitic melts and can explain the low CaO/Al_2O_3 of the magnesian andesites. While percolating through the "harzburgite passage", the produced magnesian andesites may have incorporated the forsteritic olivine xenocrysts which host MIs with variable CaO/Al_2O_3 ratios.

CRediT authorship contribution statement

Yasuhiro Hirai: Writing – review & editing, Writing – original draft, Methodology, Investigation, Funding acquisition, Formal analysis, Data curation, Conceptualization. **Yoshihiko Tamura:** Writing – review & editing, Writing – original draft, Supervision, Project administration, Funding acquisition, Conceptualization. **Takeshi Hanyu:** Writing – review & editing, Writing – original draft, Supervision, Methodology. **Qing Chang:** Writing – review & editing, Writing – original draft, Methodology, Data curation. **Christian Timm:** Writing – review & editing, Writing – original draft, Supervision. **Kaj Hoernle:** Writing – review & editing, Writing – original draft, Supervision, Funding acquisition.

Declaration of competing interest

The authors declare that they have no known competing financial interests or personal relationships that could have appeared to influence the work reported in this paper.

Data availability

All data used for the research are described in the article.

Acknowledgements

We thank the captains and crew of the R/V SONNE for their successful sampling. We thank the two anonymous reviewers for carefully reading our manuscript and for their many insightful comments and suggestions. A. Tame is thanked for analytical assistance with the EPMA measurement. This work was supported by the JSPS KAKENHI grants 19 J10691 and 24H02520 to Y. H. and JP21H01195 to Y. T. Part of this research was supported by the Environment Research and Technology Development Fund (JPMEERF20244M02) of the Environmental Restoration and Conservation Agency provided by the Ministry of the Environment of Japan. We thank the German Federal Ministry of Education and Research (BMBF) (grant no. 03G0255A) for funding the R/V SONNE SO255 cruise.

Appendix A. Supplementary data

Supplementary data to this article can be found online at https://doi.org/10.1016/j.chemgeo.2024.122218.

References

Baker, M.B., Stolper, E.M., 1994. Determining the composition of high-pressure mantle melts using diamond aggregates. Geochim. Cosmochim. Acta 58, 2811–2827. https://doi.org/https://doi.org/10.1016/0016-7037(94)90116-3.
Baker, M.B., Grove, T.L., Price, R., 1994. Primitive basalts and andesites from the Mt. Shasta region, N. California: products of varying melt fraction and water content. Contrib. Mineral. Petrol. 118, 111–129. https://doi.org/https://doi.org/10.1007/BF01052863.
Barker, S.J., Wilson, C.J.N., Baker, J.A., Millet, M.A., Rotella, M.D., Wright, I.C., Wysoczanski, R.J., 2013. Geochemistry and petrogenesis of silicic magmas in the intra-oceanic Kermadec arc. J. Petrol. 54, 351–391. https://doi.org/https://doi.org/10.1093/petrology/egs071.
Barsdell, M., 1988. Petrology and petrogenesis of clinopyroxene-rich tholeiitic Lavas, Merelava Volcano, Vanuatu. J. Petrol. 29, 927–964. https://doi.org/https://doi.org/10.1093/petrology/29.5.927.
Barsdell, M., Berry, R.F., 1990. Origin and evolution of primitive Island Arc ankaramites from Western Epi, Vanuatu. J. Petrol. 31, 747–777.
Bassett, D., Kopp, H., Sutherland, R., Henrys, S., Watts, A.B., Timm, C., Scherwath, M., Grevemeyer, I., de Ronde, C.E.J., 2016. Crustal structure of the Kermadec arc from MANGO seismic refraction profiles. J. Geophys. Res. Solid Earth 121, 7514–7546. https://doi.org/10.1002/2016JB013194.
Bédard, J.H., 2005. Partitioning coefficients between olivine and silicate melts. Lithos. https://doi.org/10.1016/j.lithos.2005.03.011.
Birner, S.K., Warren, J.M., Cottrell, E., Davis, F.A., Kelley, K.A., Falloon, T.J., 2017. Forearc peridotites from tonga record heterogeneous oxidation of the mantle following subduction initiation. J. Petrol. 58, 1755–1780. https://doi.org/10.1093/petrology/egx072.
Blatter, D.L., Carmichael, I.S.E., 1998. Plagioclase-free andesites from Zitácuaro (Michoacán), Mexico: petrology and experimental constraints. Contrib. Mineral. Petrol. 132, 121–138. https://doi.org/10.1007/s004100050411.
Bowman, E.E., Ducea, M.N., 2023. Pyroxenite melting at subduction zones. Geology 51, 383–386. https://doi.org/10.1130/g50929.1.
Bryant, J.A., Yogodzinski, G.M., Churikova, T.G., 2011. High-Mg# andesitic lavas of the Shisheisky Complex, Northern Kamchatka: Implications for primitive calc-alkaline magmatism. Contrib. Mineral. Petrol. 161, 791–810. https://doi.org/10.1007/s00410-010-0565-4.
Chen, Y., Zhang, Y., 2008. Olivine dissolution in basaltic melt. Geochim. Cosmochim. Acta 72, 4756–4777. https://doi.org/10.1016/j.gca.2008.07.014.
Chen, Y., Zhang, Y., 2009. Clinopyroxene dissolution in basaltic melt. Geochim. Cosmochim. Acta 73, 5730–5747. https://doi.org/10.1016/j.gca.2009.06.016.

Danyushevsky, L.V., Plechov, P., 2011. Petrolog3: integrated software for modeling crystallization processes. Geochem. Geophys. Geosyst. 12 https://doi.org/10.1029/2011GC003516.

Danyushevsky, L.V., Della-Pasqua, F.N., Sokolov, S., 2000. Re-equilibration of melt inclusions trapped by magnesian olivine phenocrysts from subduction-related magmas: petrological implications. Contrib. Mineral. Petrol. 138, 68–83. https://doi.org/10.1007/PL00007664.

Danyushevsky, L.V., Leslie, R.J., Crawford, A.J., Durance, P., 2004. Melt Inclusions in primitive olivine phenocrysts: the role of localized reaction processes in the origin of anomalous compositions. J. Petrol. 45, 2531–2553. https://doi.org/10.1093/petrology/egh080.

de Ronde, C.E.J., Baker, E.T., Massoth, G.J., Lupton, J.E., Wright, I.C., Sparks, R.J., Bannister, S.C., Reyners, M.E., Walker, S.L., Greene, R.R., Ishibashi, J., Faure, K., Resing, J.A., Lebon, G.T., 2007. Submarine hydrothermal activity along the mid-Kermadec Arc, New Zealand: large-scale effects on venting. Geochem. Geophys. Geosyst. 8 https://doi.org/10.1029/2006GC001495.

Della-Pasqua, F.N., Varne, R., 1997. Primitive ankaramitic magmas in volcanic arcs: a melt-inclusion approach. Can. Mineral. 35, 291–312.

Dixon, J.E., Stolper, E., Delaney, J.R., 1988. Infrared spectroscopic measurements of CO_2 and H_2O in Juan de Fuca Ridge basaltic glasses. Earth and Planetary Science Letters 90 (1), 87–104. https://doi.org/10.1016/0012-821X(88)90114-8.

Elburg, M.A., Kamenetsky, V.S., Foden, J.D., Sobolev, A., 2007. The origin of medium-K ankaramitic arc magmas from Lombok (Sunda arc, Indonesia): mineral and melt inclusion evidence. Chem. Geol. 240, 260–279. https://doi.org/10.1016/j.chemgeo.2007.02.015.

Ewart, A., Bryan, W.B., Chappell, B.W., Rudnick, R.L., 1994. 24. Regional geochemistry of the Lau-Tonga arc and backarc systems. Proc. Ocean Drill. Prog. Sci. Results 135, 385–425.

Falloon, T.J., Green, D.H., 1987. Anhydrous partial melting of MORB pyrolite and other peridotite compositions at 10 kbar: implications for the origin of primitive MORB glasses. Mineral. Petrol. 37, 181–219. https://doi.org/10.1007/BF01161817.

Falloon, T.J., Green, D.H., 1988. Anhydrous partial melting of peridotite from 8 to 35 kb and the petrogenesis of MORB. J. Petrol. Spe. 379–414 https://doi.org/10.1093/petrology/Special_Volume.1.379.

Gaetani, G.A., O'Leary, J.A., Shimizu, N., Bucholz, C.E., Newville, M., 2012. Rapid reequilibration of H_2O and oxygen fugacity in olivine-hosted melt inclusions. Geology 40, 915–918. https://doi.org/10.1130/G32992.1.

Gamble, J.A., Wright, I.C., Baker, J.A., 1993. Seafloor geology and petrology in the oceanic to continental transition zone of the Kermadec-Havre-Taupo Volcanic Zone arc system, New Zealand. N. Z. J. Geol. Geophys. 36, 417–435. https://doi.org/10.1080/00288306.1993.9514588.

Gamble, J., Woodhead, J.O.N., Wright, I.A.N., Smith, I.A.N., 1996. Basalt and sediment geochemistry and magma petrogenesis in a transect from Oceanic Island Arc to rifted continental margin arc : the Kermadec-Hikurangi Margin , SW Pacific. J. Petrol. 37, 1529–1546.

Gamble, J.A., Christie, R.H.K., Wright, I.C., Wysoczanski, R.J., 1997. Primitive K-rich magmas from Clark Volcano, southern Kermadec Arc; a paradox in the K-depth relationship. Can. Mineral. 35, 275–290.

Gavrilenko, M., Herzberg, C., Vidito, C., Carr, M.J., Tenner, T., Ozerov, A., 2016. A calcium-in-olivine geohygrometer and its application to subduction zone magmatism. J. Petrol. 57, 1811–1832. https://doi.org/10.1093/petrology/egw062.

Girona, T., Costa, F., 2013. DIPRA: a user-friendly program to model multi-element diffusion in olivine with applications to timescales of magmatic processes. Geochem. Geophys. Geosyst. 14, 422–431. https://doi.org/10.1029/2012GC004427.

Green, D.H., Falloon, T.J., 1998. Pyrolite: a ringwood concept and its current expression. In: Jacson, I. (Ed.), The Earth's Mantle: Composition, Structure, and Evolution. Cambridge University Press, pp. 311–380.

Green, D.H., Schmidt, M.W., Hibberson, W.O., 2004. Island-arc ankaramites: primitive melts from fluxed refractory lherzolitic mantle. J. Petrol. 45, 391–403. https://doi.org/https://doi.org/10.1093/petrology/egg101.

Grove, T., Parman, S., Bowring, S., Price, R., Baker, M., 2002. The role of an H_2O-rich fluid component in the generation of primitive basaltic andesites and andesites from the Mt. Shasta region, N California. Contrib. Mineral. Petrol. 142, 375–396. https://doi.org/10.1007/s004100100299.

Grove, T.L., Elkins-Tanton, L.T., Parman, S.W., Chatterjee, N., Müntener, O., Gaetani, G. A., 2003. Fractional crystallization and mantle-melting controls on calc-alkaline differentiation trends. Contrib. Mineral. Petrol. 145, 515–533. https://doi.org/10.1007/s00410-003-0448-z.

Haase, K.M., Worthington, T.J., Stoffers, P., Garbe-scho, D., Wright, I., 2002. Mantle dynamics, element recycling, and magma genesis beneath the Kermadec Arc-Havre Trough. Geochem. Geophys. Geosyst. 3, 1–22. https://doi.org/10.1029/2002GC000335.

Haase, K.M., Stroncik, N., Garbe-Schönberg, D., Stoffers, P., 2006. Formation of island arc dacite magmas by extreme crystal fractionation: an example from Brothers Seamount, Kermadec island arc (SW Pacific). J. Volcanol. Geotherm. Res. 152, 316–330. https://doi.org/10.1016/j.jvolgeores.2005.10.010.

Hart, S.R., Davis, K.E., 1978. Nickel partitioning between olivine and silicate melt. Earth Planet. Sci. Lett. 40, 203–219. https://doi.org/10.1016/0012-821X(78)90091-2.

Heyworth, Z., Turner, S., Schaefer, B., Wood, B., George, R., Berlo, K., Cunningham, H., Price, R., Cook, C., Gamble, J., 2007. ^{238}U-^{230}Th-^{226}Ra-^{210}Pb constraints on the genesis of high-Mg andesites at White Island, New Zealand. Chem. Geol. 243, 105–121. https://doi.org/10.1016/j.chemgeo.2007.05.012.

Hirai, Y., Tamura, Y., Sato, T., Miyazaki, T., Chang, Q., Vaglarov, B.S., Kimura, J.-I., Hoernle, K., Werner, R., Hauff, F., Timm, C., 2023. Magnesian andesites from Kibblewhite volcano in the Kermadec Arc, New Zealand. J. Petrol. 64, 1–23. https://doi.org/10.1093/petrology/egad060.

Hirose, K., 1997. Melting experiments on Iherzolite KLB-1 under hydrous conditions and generation of high-magnesian andesitic melts. Geology 25, 42–44. https://doi.org/10.1130/0091-7613(1997)025<0042:MEOLKU>2.3.CO.

Hirose, K., Kawamoto, T., 1995. Hydrous partial melting of lherzolite at 1 GPa: the effect of H_2O on the genesis of basaltic magmas. Earth Planet. Sci. Lett. 133, 463–473. https://doi.org/10.1016/0012-821X(95)00096-U.

Hirose, K., Kushiro, I., 1993. Partial melting of dry peridotites at high pressures: determination of compositions of melts segregated from peridotite using aggregates of diamond. Earth Planet. Sci. Lett. 114, 477–489. https://doi.org/10.1016/0012-821X(93)90077-M.

Hoernle, K., Hauff, F., Werner, R., 2017. RV SONNE Fahrtbericht/Cruise Report SO255: VITIAZ – The Life Cycle of the Vitiaz-Kermadec Arc / Backarc System: from Arc Initiation to Splitting and Backarc Basin Formation. GEOMAR Report N. Ser. 03, p. 386.

Ishii, T., Robinson, P.T., Maekawa, H., Fiske, R., 1992. Petrological studies of peridotites from diapiric serpentinite seamounts in the Izu-Ogasawara-Mariana Forearc, Leg 125. In: Proceedings of the Ocean Drilling Program, Scientific Results, pp. 445–485. https://doi.org/10.2973/odp.proc.sr.125.129.1992.

Kamenetsky, V., Métrich, N., Cioni, R., 1995. Potassic primary melts of vulsini (Roman Province): evidence from mineralogy and melt inclusions. Contrib. Mineral. Petrol. 120, 186–196. https://doi.org/https://doi.org/10.1007/BF00287116.

Kamenetsky, V.S., Zelenski, M., Gurenko, A., Portnyagin, M., Ehrig, K., Kamenetsky, M., Churikova, T., Feig, S., 2017. Silicate-sulfide liquid immiscibility in modern arc basalt (Tolbachik volcano, Kamchatka): part II. Composition, liquidus assemblage and fractionation of the silicate melt. Chem. Geol. 471, 92–110. https://doi.org/10.1016/j.chemgeo.2017.09.019.

Kelemen, P.B., 1990. Reaction between ultramafic rock and fractionating basaltic magma I. phase relations, the origin of calc-alkaline magma series, and the formation of discordant dunite. J. Petrol. 31, 51–98. https://doi.org/10.1093/petrology/31.1.51.

Kelemen, P.B., Dick, H.J.B., Quick, J.E., 1992. Formation of harzburgite by pervasive melt/rock reaction in the upper mantle. Nature 358, 635–641. https://doi.org/10.1038/358635a0.

Kent, A.J.R., 2008. Melt inclusions in basaltic and related volcanic rocks. Rev. Mineral. Geochem. 69, 273–331. https://doi.org/10.2138/rmg.2008.69.8.

Kessel, R., Schmidt, M.W., Ulmer, P., Pettke, T., 2005. Trace element signature of subduction-zone fluids, melts and supercritical liquids at 120-180 km depth. Nature 437, 724–727. https://doi.org/10.1038/nature03971.

Kogiso, T., Hirschmann, M.M., 2001. Experimental study of clinopyroxenite partial melting and the origin of ultra-calcic melt inclusions. Contrib. Mineral. Petrol. 142, 347–360. https://doi.org/10.1007/s004100100295.

Kushiro, I., 1996. Partial melting of a fertile mantle peridotite at high pressures: An experimental study using aggregates of diamond. Earth Process. 95, 109–122. https://doi.org/10.1029/GM095p0109.

Lange, R.A., Carmichael, I.S.E., 1987. Densities of Na_2O–K_2O–CaO–MgO–FeO-Fe_2O_3–Al_2O_3–TiO_2–SiO_2 liquids: new measurements and derived partial molar properties. Geochim. Cosmochim. Acta 51, 2931–2946.

Langmuir, C.H., Bézos, A., Escrig, S., Parman, S.W., 2006. Chemical systematics and hydrous melting of the mantle in back-arc basins. Geophys. Monogr. Ser. 166, 87–146. https://doi.org/10.1029/166GM07.

Laporte, D., Toplis, M.J., Seyler, M., Devidal, J.L., 2004. A new experimental technique for extracting liquids from peridotite at very low degrees of melting: application to partial melting of depleted peridotite. Contrib. Mineral. Petrol. 146, 463–484. https://doi.org/10.1007/s00410-003-0509-3.

Lloyd, A.S., Plank, T., Ruprecht, P., Hauri, E.H., Rose, W., 2013. Volatile loss from melt inclusions in pyroclasts of differing sizes. Contrib. Mineral. Petrol. 165, 129–153. https://doi.org/10.1007/s00410-012-0800-2.

McDonough, W.F., Sun, S.S., 1995. The composition of the Earth. Chem. Geol. 120, 223–253.

Médard, E., Schmidt, M.W., Schiano, P., 2004. Liquidus surfaces of ultracalcic primitive melts: formation conditions and sources. Contrib. Mineral. Petrol. 148, 201–215. https://doi.org/10.1007/s00410-004-0591-1.

Médard, E., Schmidt, M.W., Schiano, P., Ottolini, L., 2006. Melting of amphibole-bearing wehrlites: an experimental study on the origin of ultra-calcic nepheline-normative melts. J. Petrol. 47, 481–504. https://doi.org/10.1093/petrology/egi083.

Métrich, N., Deloule, E., 2014. Water content, δD and δ11B tracking in the Vanuatu arc magmas (Aoba Island): insights from olivine-hosted melt inclusions. Lithos 206–207, 400–408. https://doi.org/10.1016/j.lithos.2014.08.011.

Mitchell, A.L., Grove, T.L., 2015. Melting the hydrous, subarc mantle : the origin of primitive andesites. Contrib. Mineral. Petrol. 170, 1–23. https://doi.org/10.1007/s00410-015-1161-4.

Miyashiro, A., 1974. Volcanic rock series in island arcs and active continental margins. Am. J. Sci. 274, 321–355. https://doi.org/10.2475/ajs.274.4.321.

Morgan, G.B., London, D., 1996. Optimizing the electron microprobe analysis of hydrous alkali aluminosilicate glasses. Am. Mineral. 81, 1176–1185. https://doi.org/10.2138/am-1996-9-1016.

Nichols, A.R.L., Wysoczanski, R.J., 2007. Using micro-FTIR spectroscopy to measure volatile contents in small and unexposed inclusions hosted in olivine crystals. Chem. Geol. 242, 371–384. https://doi.org/10.1016/j.chemgeo.2007.04.007.

Nishizawa, T., Nakamura, H., Churikova, T., Gordeychik, B., Ishizuka, O., Haraguchi, S., Miyazaki, T., Vaglarov, B.S., Chang, Q., Hamada, M., Kimura, J.I., Ueki, K., Toyama, C., Nakao, A., Iwamori, H., 2017. Genesis of ultra-high-Ni olivine in high-Mg andesite lava triggered by seamount subduction. Sci. Rep. 7, 1–11. https://doi.org/10.1038/s41598-017-10276-3.

Pickering-Witter, J., Johnston, A.D., 2000. The effects of variable bulk composition on the melting systematics of fertile peridotitic assemblages. Contrib. Mineral. Petrol. 140, 190–211. https://doi.org/10.1007/s004100000183.

Portnyagin, M.V., Plechov, P.Yu., Matveev, S.V., Osipenko, A.B., Mironov, N.L., 2005. Petrology of avachites, high-magnesian basalts of Avachinsky volcano, Kamchatka: I. General characteristics and composition of rocks and minerals. Petrologiya 13, 99–121.

Portnyagin, M., Mironov, N., Botcharnikov, R., Gurenko, A., Almeev, R.R., Luft, C., Holtz, F., 2019. Dehydration of melt inclusions in olivine and implications for the origin of silica-undersaturated island-arc melts. Earth Planet. Sci. Lett. 517, 95–105. https://doi.org/10.1016/j.epsl.2019.04.021.

Ruscitto, D.M., Wallace, P.J., Kent, A.J.R., 2011. Revisiting the compositions and volatile contents of olivine-hosted melt inclusions from the Mount Shasta region: implications for the formation of high-Mg andesites. Contrib. Mineral. Petrol. 162, 109–132. https://doi.org/10.1007/s00410-010-0587-y.

Schiano, P., Eiler, J.M., Hutcheon, I.D., Stolper, E.M., 2000. Primitive CaO-rich, silica-undersaturated melts in island arcs: evidence for the involvement of clinopyroxene-rich lithologies in the petrogenesis of arc magmas. Geochem. Geophys. Geosyst. 1 https://doi.org/10.1029/1999gc000032.

Schmidt, M.W., Green, D.H., Hibberson, W.O., 2004. Ultra-calcic magmas generated from Ca-depleted mantle: an experimental study on the origin of Ankaramites. J. Petrol. 45, 531–554. https://doi.org/10.1093/petrology/egg093.

Sobolev, A.V., Hofmann, A.W., Sobolev, S.V., Nikogosian, I.K., 2005. An olivine-free mantle source of Hawaiian shield basalts. Nature 434, 590–597. https://doi.org/10.1038/nature03411.

Sobolev, A.V., Hofmann, A.W., Kuzmin, D.V., Yaxley, G.M., Arndt, N.T., Chung, S.-L., Danyushevsky, L.V., Elliott, T., Frey, F.A., Garcia, M.O., Gurenko, A.A., Kamenetsky, V.S., Kerr, A.C., Krivolutskaya, N.A., Matvienkov, V.V., Nikogosian, I. K., Rocholl, A., Sigurdsson, I.A., Sushchevskaya, N.M., Teklay, M., 2007. The amount of recycled crust in sources of mantle-derived melts. Science 1979 (316), 412–417.

Sorbadere, F., Schiano, P., Métrich, N., Garaebiti, E., 2011. Insights into the origin of primitive silica-undersaturated arc magmas of Aoba volcano (Vanuatu arc). Contrib. Mineral. Petrol. 162, 995–1009. https://doi.org/10.1007/s00410-011-0636-1.

Sorbadere, F., Schiano, P., Métrich, N., 2013. Constraints on the origin of nepheline-normative primitive magmas in Island arcs inferred from olivine-hosted melt inclusion compositions. J. Petrol. 54, 215–233. https://doi.org/10.1093/petrology/egs063.

Straub, S.M., LaGatta, A.B., Martin-Del Pozzo, A.L., Langmuir, C.H., 2008. Evidence from high-Ni olivines for a hybridized peridotite/pyroxenite source for orogenic andesites from the central Mexican Volcanic Belt. Geochem. Geophys. Geosyst. 9 https://doi.org/10.1029/2007GC001583.

Straub, S.M., Gomez-tuena, A., Stuart, F.M., Zellmer, G.F., Espinasa-perena, R., Cai, Y., Iizuka, Y., 2011. Formation of hybrid arc andesites beneath thick continental crust. Earth Planet. Sci. Lett. 303, 337–347. https://doi.org/10.1016/j.epsl.2011.01.013.

Straub, S.M., Zellmer, G.F., Gómez-Tuena, A., Espinasa-Pereñ, A.R., Martin-Del Pozzo, A. L., Stuart, F.M., Langmuir, C.H., 2014. A genetic link between silicic slab components and calc-alkaline arc volcanism in central Mexico. Geol. Soc. Spec. Publ. 385, 31–64. https://doi.org/10.1144/SP385.14.

Sugawara, T., 2000. Empirical relationships between temperature, pressure, and MgO content in olivine and pyroxene saturated liquid. J. Geophys. Res. Solid Earth 105, 8457–8472. https://doi.org/10.1029/2000JB900010.

Sun, S.S., McDonough, W.F., 1989. Chemical and isotopic systematics of oceanic basalts: implications for mantle composition and processes. Geol. Soc. Lond., Spec. Publ. 42, 313–345. https://doi.org/10.1144/GSL.SP.1989.042.01.19.

Tamura, Y., Ishizuka, O., Stern, R., Nichols, A.R.L., Kawabata, H., Hirahara, Y., Chang, Q., Miyazaki, T., Kimura, J.I., Embley, R.W., Tatsumi, Y., 2014. Mission Immiscible: distinct subduction components generatetwo primary magmas at Pagan Volcano, Mariana Arc. J. Petrol. 55, 63–101. https://doi.org/10.1093/petrology/egt061.

Tamura, Yoshihiko, Ishizuka, O., Sato, T., Nichols, A.R.L., 2019a. Nishinoshima volcano in the Ogasawara Arc: new continent from the ocean? Island Arc 28, 1–20. https://doi.org/10.1111/iar.12285.

Tamura, Y., Sato, T., Ishizuka, O., Hirai, Y., Miyazaki, T., 2019b. ANANBA (Ankaramite-Andesite-Basalt) model of the evolution of oceanic Arc Volcanoes. Abstr. Am. Geophys. Union Fall Meet. 2019, V51G–0207.

Tatsumi, Y., Ishizaka, K., 1982. Origin of high-magnesian andesites in the Setouchi volcanic belt, southwest Japan, I. Petrographical and chemical characteristics. Earth Planet. Sci. Lett. 60, 293–304. https://doi.org/10.1016/0012-821X(82)90008-5.

Timm, C., Davy, B., Haase, K., Hoernle, K.A., Graham, I.J., de Ronde, C.E.J., Woodhead, J., Bassett, D., Hauff, F., Mortimer, N., Seebeck, H.C., Wysoczanski, R.J., Caratori-Tontini, F., Gamble, J.A., 2014. Subduction of the oceanic Hikurangi Plateau and its impact on the Kermadec arc. Nat. Commun. 5, 4923. https://doi.org/10.1038/ncomms5923.

Timm, C., Leybourne, M.I., Hoernle, K., Wysoczanski, R.J., Hauff, F., Handler, M., Tontini, F.C., de Ronde, C.E.J., 2016. Trench-perpendicular geochemical variation between two adjacent Kermadec arc volcanoes Rumble II East and West: the role of the subducted Hikurangi Plateau in element recycling in arc magmas. J. Petrol. 57, 1335–1360. https://doi.org/10.1093/petrology/egw042.

Turner, S., Hawkesworth, C., Rogers, N., Bartlett, J., Worthington, T., Hergt, J., Pearce, J., Smith, I., 1997. ^{238}U-^{230}Th disequilibria, magma petrogenesis, and flux rates beneath the depleted Tonga-Kermadec island arc. Geochim. Cosmochim. Acta 61, 4855–4884. https://doi.org/10.1016/S0016-7037(97)00281-0.

Villiger, S., Ulmer, P., Müntener, O., Thompson, A., 2004. The liquid line of descent of anhydrous, mantle-derived, tholeiitic liquids by fractional and equilibrium crystallization–an experimental study at 1.0 GPa. J. Petrol. 45, 2369–2388. https://doi.org/10.1093/petrology/egh042.

Wallace, P.J., Kamenetsky, V.S., Cervantes, P., 2015. Special collection: glasses, melts, and fluids, as tools for understanding volcanic processes and hazards. Melt inclusion CO<inf>2</inf> contents, pressures of olivine crystallization, and the problem of shrinkage bubbles. Am. Mineral. 100, 787–794. https://doi.org/10.2138/am-2015-5029.

Wasylenki, L.E., Baker, M.B., Kent, A.J.R., Stolper, E.M., 2003. Near-solidus melting of the shallow upper mantle: partial melting experiments on depleted peridotite. J. Petrol. 44, 1163–1191. https://doi.org/10.1093/petrology/44.7.1163.

Wood, B.J., Turner, S.P., 2009. Origin of primitive high-Mg andesite: constraints from natural examples and experiments. Earth Planet. Sci. Lett. 283, 59–66. https://doi.org/10.1016/j.epsl.2009.03.032.

Wright, I.C., Worthington, T.J., Gamble, J.A., 2006. New multibeam mapping and geochemistry of the 30°-35° S sector, and overview, of southern Kermadec arc volcanism. J. Volcanol. Geotherm. Res. 149, 263–296. https://doi.org/10.1016/j.jvolgeores.2005.03.021.

Wysoczanski, R.J., Handler, M.R., Schipper, C.I., Leybourne, M.I., Creech, J., Rotella, M. D., Nichols, A.R.L., Wilson, C.J.N., Stewart, R.B., 2012. The tectonomagmatic source of ore metals and volatile elements in the Southern Kermadec Arc. Econ. Geol. 107, 1539–1556. https://doi.org/10.2113/econgeo.107.8.1539.

Yogodzinski, G.M., Volynets, O.N., Koloskov, A.V., Seliverstov, N.I., Matvenkov, V.V., 1994. Magnesian andesites and the subduction component in a strongly calc-alkaline series at Piip volcano, far western Aleutians. J. Petrol. 35, 163–204. https://doi.org/10.1093/petrology/35.1.163.